nature communications



Article

https://doi.org/10.1038/s41467-025-60451-8

Longitudinal changes in brain asymmetry track lifestyle and disease

Received: 1 August 2024

Accepted: 22 May 2025

Published online: 01 July 2025

Check for updates

Karin Saltoun ^{1,2}, B. T. Thomas Yeo ^{3,4,5,6,7,8}, Lynn Paul ⁹, Jorn Diedrichsen ¹⁰ & Danilo Bzdok ^{1,2} □

Human beings may have evolved the largest asymmetries of brain organization in the animal kingdom. Hemispheric left-vs-right specialization is especially pronounced in species-unique capacities, including emotional processing such as facial judgments, language-based feats such as reading books, and creativity such as musical performances. We hence chart the largest longitudinal brain-imaging resource, and provide evidence that brain asymmetry changes continuously in a manner suggestive of neural plasticity throughout adulthood. In the UK Biobank population cohort, we demonstrate that wholebrain patterns of asymmetry changes show robust phenome-wide associations across 959 distinct variables spanning 11 categories. We also find that changes in brain asymmetry over years co-occur with changes among specific lifestyle markers. We uncover specific brain asymmetry changes which systematically co-occur with entering a new phase of life, namely retirement. Finally, we reveal relevance of evolving brain asymmetry within subjects to major disease categories across ~4500 total medical diagnoses. Our findings speak against the idea that asymmetrical neural systems are conserved throughout adulthood.

It is hard to dispute that the brain has a role in controlling behaviour. Equally established is that both behaviour and environment led to deep structural adaptations in neural circuits¹. This interdependence between brain and lifestyle is perhaps not restricted to a critical period in early life. Rather, behavioural experiences influence brain structure throughout the lifespan^{2,3}. Indeed, within-individual changes in brain architecture, as captured through structural brain scanning (T1weighted MRI), can be observed after only 12 weeks of juggling practice in young adults⁴, and middle-aged persons (mean age 60)³. Over the span of weeks, regular practice of complex whole-body balancing tasks resulted in increased grey matter volume in left hemispheric regions, including supplementary motor area, and medial orbitofrontal cortex; alongside simultaneous reductions in grey matter volumes in the right hemisphere, including right putamen, inferior orbitofrontal cortex and middle temporal gyrus⁵. In less than an hour of training, unskilled individuals learning to play piano exhibited taskspecific structural modifications in diffusivity measures (DW-MRI) in the left premotor area and left middle temporal gyrus⁶. Recent work has also advocated for the necessity/utility of dedicated longitudinal analyses to understand lifelong neuroplasticity, owing to the tendency

¹The Neuro - Montreal Neurological Institute (MNI), McConnell Brain Imaging Centre, Department of Biomedical Engineering, Faculty of Medicine, School of Computer Science, McGill University, Montreal, Canada. 2Mila - Quebec Artificial Intelligence Institute, Montreal, QC, Canada. 3Centre for Sleep and Cognition & Centre for Translational MR Research, Yong Loo Lin School of Medicine, National University of Singapore, Singapore, Singapore. ⁴Department of Medicine, Human Potential Translational Research Programme & Institute for Digital Medicine (WisDM), Yong Loo Lin School of Medicine, National University of Singapore, Singapore, Singapore. ⁵Department of Electrical and Computer Engineering, National University of Singapore, Singapore, Singapore. ⁶N.1 Institute for Health, National University of Singapore, Singapore, Singapore. 7Inntegrative Sciences and Engineering Programme (ISEP), National University of Singapore, Singapore, Singapore. 8Martinos Center for Biomedical Imaging, Massachusetts General Hospital, Charlestown, MA, USA. 9Division of the Humanities and Social Sciences, California Institute of Technology, Pasadena, CA, USA. 10 Western Institute of Neuroscience, Western University, London, Ontario, Canada. e-mail: bzdokdan@mila.guebec

of cross-sectional models to underestimate individual-level brain changes⁷.

Behaviour-induced changes in adult brain structure are also evident in cognitive domains beyond motor capacities^{1,8,9}. For example, both meta-cognition and language skills are responsive to regular active training. One month of mindfulness training resulted in withinindividual white-matter changes in adults, including in the corpus callosum - the largest axon fiber connection between the left and right hemisphere¹⁰. Investigations conducted on identical twins showed strong evidence that white-matter structure inside the corpus callosum can be altered by specific environmental, rather than just genetic, factors¹¹. Introduction of new lexical terms into the vocabulary of young adults was observed to induce diffusion-related structural modifications of cortical language areas, including left inferior frontal gyrus, left middle temporal gyrus, and left inferior parietal lobule¹². These examples illustrate behaviour-induced adaptations within the brain that involve both asymmetrical structural changes as well as alterations in the corpus callosum - the primary channel for information transfer between both brain hemispheres¹³.

Habits and other recurring behaviours in humans probably entail distinct manifestations in the brain. Empathy is an evolved interpersonal capacity which can broadly be distinguished into cognitive (1 understand what you feel') and emotional ('I feel what you feel') empathy¹⁴. Over the course of weeks, regular participation in training modules specifically designed to target and improve only one of these two different empathy systems resulted in longitudinal structural grey matter changes specific to the trained empathy system. Improvements in cognitive empathy cooccurred with measurable changes in right middle temporal gyrus and left ventrolateral prefrontal cortex, but not their contralateral homologues. Conversely, training in emotional empathy related to structural changes in regions including right supramarginal gyrus, involved in language, right insular-opercular regions, and left posterior cingulate cortex¹⁵. Rather, behavioural experiences influence brain structure throughout the lifespan^{2,3}. Further. language, in addition to being among the most sophisticated cognitive processes in humans, exhibits large degrees of asymmetrical brain specialisation¹⁶. In fact, in teenagers, growing proficiency in a second language occurring over the course of months was related to within-subject changes in grey matter density in left inferior frontal gyrus and left anterior temporal lobe¹⁷. Notably, absolute grey matter density was not linked to absolute language proficiency at any single time point, suggesting brain structure changes reflect language learning experiences, regardless of whether brain structure itself is associated with individual language skill¹⁷. Plastic changes in the brain are thus likely to be specific to evolving mental capacities and may be sensitive to changes in a specific ability, with and without sensitivity to the initial performance.

Asymmetric lateralisation of neurocognitive processes is a defining feature of many advanced mental abilities¹⁶. Observed structural brain changes tie into lateralized cognitive functions such as language¹², and may preferentially implicate one hemisphere over the other^{5,15,17}. In semantic dementia, the impacted hemisphere affects the type and degree of incurred cognitive deficits18. The association between cognitive impairment and localised regional structure measurements has previously been shown to be captured by the relative hemispheric balance between left-right homologues and not the total structural volume of either region of a pair¹⁹. As dementias progress, local asymmetries become more pronounced while remaining directionally stable^{20,21}. However, across the human population, there is a co-existence between instances of both greater left hemisphere impact and greater right hemisphere impact¹⁸. Therefore, aggregating across these instances of greater left hemisphere changes and greater right hemisphere changes may suggest that there is no preferred direction of change across individuals²¹. Nevertheless, hemispherical asymmetries exist on an individual level and may lead to untapped insight into the progression of major brain diseases.

Hippocampal asymmetry and its association with cognitive decline serves as a fruitful window into the interplay between structural asymmetry and relevant behavioural measures. Zooming into this region and its asymmetry, researchers have found that the magnitude of hippocampal volume asymmetry increases with increasing severity of diagnosis (cognitively normal, stable and progressive mild cognitive impairment, and Alzheimer's disease)22. Another exploration of asymmetry of hippocampal morphological shape separately analysed both amount of asymmetry (absolute hemispheric difference) and direction of asymmetry (hemispheric difference). The authors found dementia diagnoses were more strongly associated with absolute hemispheric differences than with directional hemispheric differences²¹. The authors attributed this to the lack of a dominant direction of hemispheric asymmetry across the population²¹. In a separate analysis, the group found longitudinal intraindividual factors captured two to five times more structural asymmetry change than cross-sectional age effects²¹. This finding is consistent with the results of a more recent comparison of longitudinal versus cross-sectional brain trajectories, which found cross-sectional estimates of rate of change are insufficient to describe known longitudinal rates of brain change over time⁷. Of importance for the present investigation, the authors argue that individual behavioural and cognitive measures may play a larger role than age in capturing observed brain feature changes⁷.

Mechanistically, macroscopic changes observed through MRI can reflect a broad array of microstructural plasticity changes²³. Invasive histological studies are largely limited to animal models and are ultimately necessary to link brain-imaging-derived measures of change to underlying cellular architecture^{1,24}. Though few in number, existing histological studies in rats, mice, and monkeys pinpoint clear cellular substrates to observed longitudinal changes in MRI signals¹. Mice trained on different kinds of the Morris water maze, each exercising different problem-solving and navigational skills, showed structural enlargement revealed by MRI in the corpus callosum, striatum, and hippocampus. Each mouse training group exhibited distinct patterns of structural changes relevant to the cognitive approach to navigating their version of the water maze. Histological staining on these same mice after training showed that morphological brain changes coincide with GAP-43 protein expression, implicated in neural remodelling - a crucial component of the presynaptic terminal and axonal growth cones²⁵. In another study on experimentally structured experience, rats which learned the location of a hidden platform in a water maze exhibited changes in fractional anisotropy (FA), a diffusion MRIderived measure capturing white matter integrity, in the corpus callosum that was unseen in rats swimming in a water maze with no hidden platform. Histological staining revealed that changes in FA in the corpus callosum were associated with increased expression of myelin basic protein, a proxy of myelination, but not astrocyte, dendritic or synaptic markers. GAP-43 staining was not conducted in this experiment²⁶. Across-species investigations using comparable training programmes for humans and rats revealed similar longitudinal structural changes across species after completion of experimental tasks on short-term learning²⁷. The magnitude of changes was associated with improvement in task performance, and histological staining in rats revealed changed expression of neuronal growth factors (BDNF) - encouraging growth and differentiation of new neurons and synapses - and synaptophysin, one of the most abundant synaptic vesicle membrane proteins, specifically in brain regions exhibiting structural changes²⁷. Converging evidence thus suggests that macroscopic structural changes observed through MRI at different time scales can reflect cellular changes associated with synaptic vesicle formation and uptake, neuronal remodelling, and mvelination.

Thus far, studies on structural plasticity in both humans and model species have largely relied on targeted laboratory interventions to assess the relationship between pre-selected cognitive functions and brain structure. A strength of structural imaging is its ability to link individual's lifestyle and behaviour traits in an ecologically valid environment, that is, outside of the MRI, to structural changes observed in MRI imaging⁹. Moreover, while brain plasticity has been reported to occur over the span of weeks^{3,4}, sometimes days⁵, and even hours^{6,12}, structural changes may persist over the course of years. Therefore, we propose an alternative approach to carefully controlled (curated) laboratory training modules towards naturalistic investigations into lifestyle events and habits and their correlates with withinindividual changes. To this end, we leveraged the UKBB resource, which combines high-quality brain scans with concurrent real-world phenotyping measures of unprecedented depth. We adopted previously delineated patterns of brain asymmetry, which encapsulate consistent brain-global motifs of structural asymmetry, as derived from careful examination of the brains of over 37,000 individuals²⁸. We examine how the extent and expression of these brain asymmetry patterns change over the span of years in individuals. We capitalised on concurrent brain imaging and behavioural phenotyping collected across years within the same individuals to specifically investigate how changes in global brain asymmetry, rather than global brain volume, relate to 977 demographic factors, behavioural measures, and phenotypic characteristics across 11 domains. We further investigated how brain asymmetry changes relate to lifestyle and behavioural changes across 9 domains that co-occur alongside our discovered brain asymmetry changes. In a multi-method approach, we consider both directional changes and absolute amounts of longitudinal brain asymmetry change across multiple brain asymmetry patterns, each of which individually captures distinct aspects of global brain asymmetry. Finally, by linking brain asymmetry to 4448 total medical health record items, we related brain asymmetry changes to several important health outcomes.

Results

The left and right brain hemispheres longitudinally change at different rates

Many advanced, human-defining cognitive abilities exhibit asymmetric organisation in the left versus right brain¹⁶. Based on some early cues in the literature, the structure of the brain may plastically respond to cognitive train in hemispherically-imbalanced and task-specific manners¹⁵. Here, we tested the possibility of longitudinal progression of brain asymmetry, alongside its associations with real-world lifestyle phenotypes. The present investigation adopts our recently established whole-brain asymmetry patterns, which capture concurrent left-right deviations in tandem with one another across the cross-sectional cohort of ~37,000 individuals in the UKBB cohort²⁸. The examination of the structural asymmetries unveiled 33 consistent patterns of structural asymmetry, which implicate distinct sets of brain features from across the brain - including white matter tracts, subcortical structures, and cerebellar lobules; collected using T1-weighted and diffusion-weighted MRI imaging²⁸. These asymmetry patterns highlight brain features whose structural asymmetries are consistently correlated to one another across the population. In this work, we extended our investigation beyond the snapshot in time afforded by previous crosssectional analysis into a longitudinal examination into if and how structural asymmetry evolves over time within individuals (Fig. 1A).

To this end, we used the full subset of UKBB subjects with two braining regions of 1425 individuals (49% male; 27.4 ± 1.4 months between visits; 62.5 ± 7.2 years old at first imaging visit). As a preliminary analysis, we probed for the possibility of unequal structural changes between pairs of homologous grey matter volumes. Through assessing regional volumes across time, we found that yearly volumetric change in

homologous grey matter regions only track each other incompletely over the years. Across 55 homologous grey matter pairs, the volume change over time in the left homologue was not perfectly correlated with the volume change over time in the right homologue (r = 0.34 (mean), ranging from 0.10 to 0.70; p <0.01 for all 55 grey matter regions; (absolute) Cohen's d = 0.82 (mean) ranging from 0.007 to 2.50). The lack of full correspondence between longitudinal volumetric changes in homologous pairs (i.e., rates of change were unequal between left and right hemisphere homologues) suggests that longitudinal change in grey matter brain structure is a non-symmetric phenomenon.

Motivated by the observation of hemispherically-diverging rate of longitudinal change, as well as the recently established knowledge that brain asymmetry is a global rather than local phenomenon²⁸, we elected to investigate structural brain asymmetry through the lens of whole-brain structural asymmetry patterns (Fig. 1A). These asymmetry patterns holistically combine structural asymmetries from across the brain into composite measures which delineate specific motifs of structural asymmetry which respects the natural interconnectedness of brain regions²⁸. To begin our investigation, we computed the expressions of all brain asymmetry patterns for all individuals with two time points using our publicly available asymmetry pattern definitions²⁸. Each asymmetry pattern characterises a unique and consistent way in which brain hemispheres are structurally dissimilar from one another. Mathematically, asymmetry pattern definitions consolidate regional structural asymmetries, represented by lateralisation indices ($LI = \frac{V_R - V_L}{0.5 * (V_R + V_L)}$), of 85 brain features (spanning 9 cerebellar lobes, 21 white matter tracts, 48 cortical grey matter regions, and 7 subcortical grey matter regions). These 85 constituent brain features combine, in accordance to previously-established asymmetry pattern definitions²⁸, into a single value which captures the expression level of a single asymmetry pattern (Fig. 1B and Supplementary Table 1). More information detailing specific asymmetry pattern properties is available in Saltoun et al. 28, and the construction of asymmetry patterns is summarized in the methods section "Construction of Asymmetry Patterns".

Once the expression of asymmetry patterns was acquired for both time points, a comparison across time in was conducted to examine if and how whole-brain asymmetry shifts in individuals across time. We take heed of previous studies indicating a lack of preferentially impacted hemisphere in some forms of brain atrophy²¹, we elected to describe structural asymmetry trajectories with two complementary measures of change. Namely, we concurrently investigated both lateralized brain asymmetry changes (LBACs) and absolute magnitude of brain asymmetry change (MBAC)s. LBACs are measured as $LBAC_k = \frac{P_{k_2} - P_{k_1}}{\Delta t}$ where P_{k_t} indicates asymmetry pattern expression at timepoints 1 (P_{k_1}) and 2 (P_{k_2}) and k indicates a particular asymmetry pattern k. LBACs captured consistent brain asymmetry changes across the population and are sensitive to instances where the hemisphere undergoing faster rate of longitudinal change for a particular homologous pair is shared across the population For example, the planum temporale is heavily implicated in asymmetry pattern 2, and may undergo imbalanced structural change over time If, across the population, the volume of the right planum temporale shrinks at a more rapid rate as compared to the left planum temporale, the observed asymmetry pattern 2 LBAC would be large indicating more extreme leftward planum temporale asymmetry at the follow-up timepoint. On the other hand, MBAC, measured as $MBAC_k = \frac{|P_{k_2} - P_{k_1}|}{\Lambda t}$, which capture the amount of asymmetry change independent of direction, are suited to capturing hemispherically-unmatched rates of change, even when distinct directions of asymmetry change co-occur across the population. Thus, if half of the population exhibits longitudinal increase of leftward asymmetry and the other half of the population exhibits similar increases in rightward asymmetry, the LBACs would be small

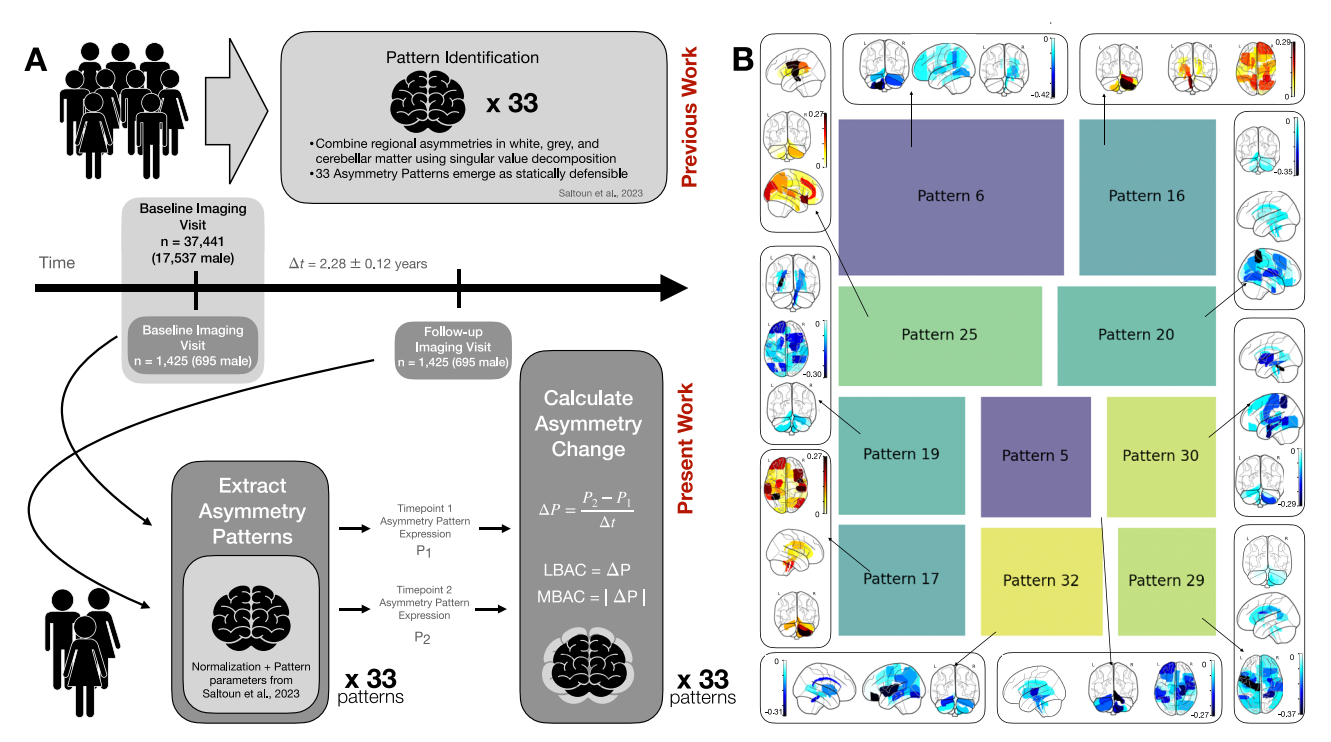


Fig. 1 | **Systematic longitudinal changes occur in multiple structural whole-brain asymmetry patterns spanning white matter, cerebellum, and cortical structures.** A Previously established whole-brain asymmetry patterns enable investigation into structural brain asymmetry change. Structural asymmetry patterns describe concurrent left-right deviations across white matter, cerebellum, and cortical structures. These asymmetry patterns have previously been discovered and delineated in work by Saltoun and colleagues (2023). We apply these established asymmetry pattern definitions²⁸ to extract measures of structural asymmetry for individuals across multiple imaging visits, with an average of over 2 years between visits. Comparing asymmetry pattern expression between timepoints in an individual enables two complementary viewpoints of structural brain asymmetry change in adults. The magnitude of brain asymmetry change (MBAC) captures how much the structural imbalance between hemispheres progressed in individuals. Longitudinal Brain Asymmetry Change (LBAC) captures how structural imbalance between hemisphere

showcases greater change. **B** Asymmetry patterns exhibiting large asymmetry changes across the population draw upon distinct combinations of brain features spanning the whole brain. Shows brain feature contributions of the 10 asymmetry patterns with the largest LBACs (border). The square size (center) represents the relative amount of change amongst the top 10 patterns encapsulated by the given asymmetry pattern. Brain maps show cortical and subcortical, major white matter tracts, and cerebellum contributions to the specified asymmetry pattern. Brain features shown on the right hemisphere represent right hemisphere homologues exhibiting larger longitudinal shifts than left hemisphere counterparts in the positive direction, and the reversed configuration in the negative direction. Asymmetry patterns with negative mean directional change (LBAC) are illustrated with blue coloured brain maps. This corresponds to the reversed configuration of brain feature changes as delineated above, with brain features shown on the right hemisphere exhibiting either diminished R > L asymmetry or increased L > R asymmetry with time. Source data are provided as a Source Data file.

(suggesting that the rate of change in the left and right hemispheres are similar). Yet, on the individual level, there is consistent skewing in one or the other direction. This would result in a measurable MBAC without a corresponding LBAC effect, highlighting the necessity of indexing change through both LBAC and MBAC. In the following, we will report both LBACs and MBACs as yearly rate of change.

By construction, our measures of longitudinal asymmetry change (LBAC and MBAC) combined changes across different levels of brain organisation, including cerebellar tissue, white matter tracts, and cortical and subcortical volumes. To aid interpretation, we related all LBACs to relative right versus left grey matter change. Based on evidence that the onset of age-related volume change is earlier in grey matter than in white matter²⁹, we calculated a reference measure which captures which hemisphere exhibited larger cortical grey matter decline. To do so, the yearly rate of change in cortical grey matter in the left (ΔG_l) and right hemisphere (ΔG_R) was computed, at which point the difference between observed volumetric change across hemispheres ($\Delta G_R - \Delta G_I$) revealed which hemisphere exhibited faster volume changes. We find a common overall trend of volume declines, rather than volume gains, across the population for both hemispheres, with the right hemisphere exhibiting slightly slower volume declines ($\Delta G_R = -1243 \pm 69 \text{ mm}^3 / \text{ year}$; standard error of mean (SEM)) than the left hemisphere (ΔG_I = -1328 ± 64 mm³ / year; SEM). To relate the overall cortical change to the LBACs, we computed a Pearson correlation coefficient between LBACs and hemisphere preferential longitudinal cortical volume change (cf. "Methods"). Through this, we ensured that positive LBACs correspond to the left hemisphere getting smaller faster than the right hemisphere.

Distinct whole-brain asymmetry patterns show unique changes over several years

We found that structural brain asymmetry is not static in adults from our UK Biobank cohort, with most asymmetry patterns (28 / 33 examined patterns) exhibiting robust LBACs over time (Fig. 2A). While 5 out of the top 10 asymmetry patterns with the largest LBACs also were among the 10 patterns with the largest MBACs, mean LBACs were relatively small compared to mean MBACs. This suggests that although individual brains change a lot in their asymmetry, across the population there may be a less consistent direction which becomes relatively (L vs R) larger or smaller - this observation underscored the value of probing complementary notions of asymmetry change. Indeed, all patterns showed salient MBACs, even asymmetry patterns with no mean change in LBAC across the population. As a specific example, asymmetry pattern 21, which combines ipsilateral middle frontal gyrus and amygdala shifts with contralateral shifts in paracingulate gyrus and corticospinal tract, exhibited a mean LBAC consistent with zero across the population. This isolated observation may be taken to suggest that this particular asymmetry pattern exhibits modest longitudinal changes towards a particular hemisphere. However, this same asymmetry

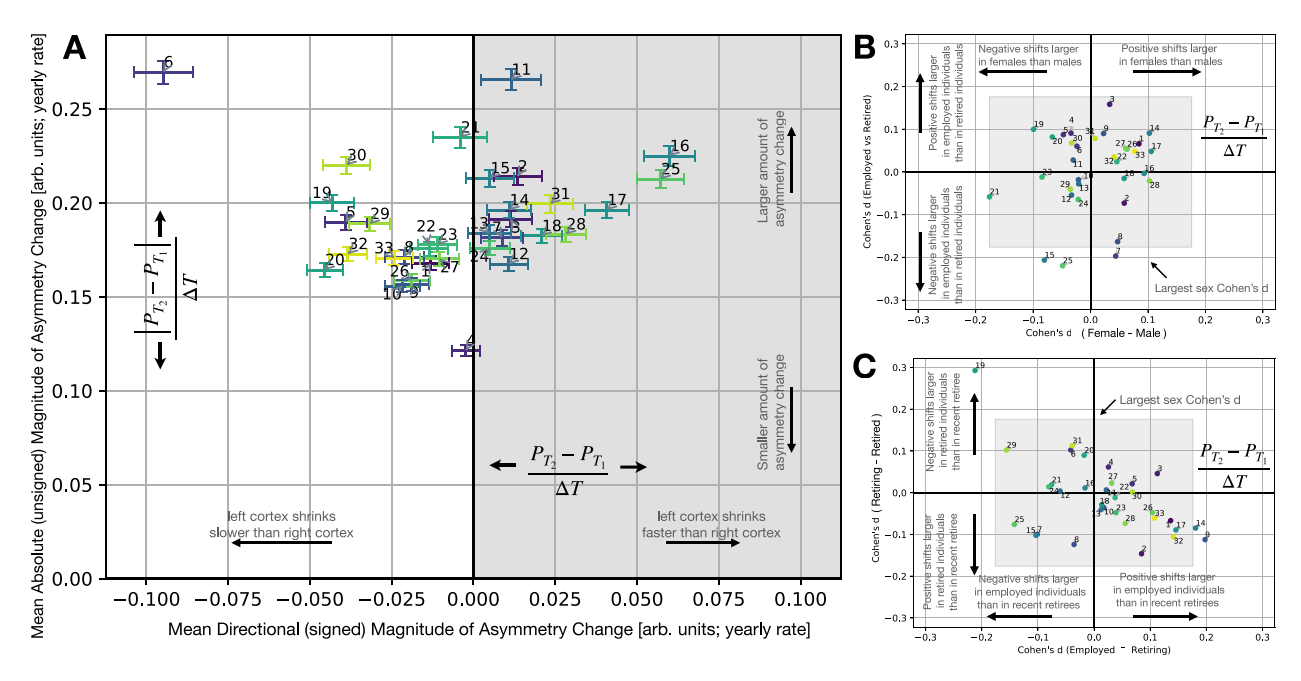


Fig. 2 | **Major lifestyle events are reflected in longitudinal progression of structural whole-brain asymmetry patterns.** A Two measures of structural brain asymmetry change both showcase relevant longitudinal progression. The amount of asymmetry change (MBAC) captures how much the structural imbalance between hemispheres progressed, regardless of direction. Asymmetry change (LBAC) captures how structural imbalance between hemispheres progresses, including which hemisphere showcases greater change. Mean LBAC and MBAC across all 33 statistically robust asymmetry patterns are shown. Error bars represent the standard error of the mean. All asymmetry patterns concurrently consider brain features spanning cortical and subcortical grey matter, major white matter tracts, and cerebellar grey and white matter. All LBACs were compared in terms of relative right versus left grey matter cortical change to aid in interpretation. This composite

reference measure tracks aggregate cortical asymmetry change but does not reflect the hemispheric bias of any individual grey matter homologue, or the hemispheric biases of cerebellum or white matter tracts. **B**, **C** The (Cohen's d) effect of retirement status across multiple separate patterns is larger than the (Cohen's d) effect of the pattern with the largest sex effect. Cohen's d effect size of LBACs between sex or employment contrasts. Three employment Cohen's d contrasts were conducted per asymmetry pattern, comparing participants who were in full-time employment at both time points (employed), in retirement at both time points (retired) or transitioned from full-time employment at the first imaging visit to retired at the second imaging visit (retiring). Grey rectangle indicates the single largest absolute Cohen's d for sex-contrast (pattern 21, |d| = 0.176). Source data are provided as a Source Data file.

pattern (21) displayed the third largest MBAC amongst all our studied asymmetry patterns. Therefore, though *individually* this measure of asymmetry changes significantly with time, across the population, there are individuals whose asymmetry pattern moves in the opposite direction.

Appreciate that our LBACs did not capture total hemispheric volume decline or gain. Rather, the grey/white matter imbalances between hemispheric homologues across the whole brain and the way in which these left-right deviations progress with time within individuals.

MBACs revealed the overall amount of longitudinal change in structural hemispheric imbalance. As indicated by its small MBAC, asymmetry was most stable for pattern 4 (Fig. 2A), which highlights several language-related brain regions, such as the planum temporale, inferior frontal gyrus, and pars triangularis. Pattern 4 was characterised by asymmetrical bias to the same hemisphere in inferior frontal gyrus, pars triangularis and frontal operculum cortex alongside asymmetries which favour the contralateral hemisphere in planum polare and central opercular cortex. Furthermore, LBAC for pattern 4 overlapped with zero, indicating there is no preferred direction of asymmetry change for this pattern across the population.

In contrast, pattern 6 had the most plastic asymmetry with time, as indicated by its large MBAC (Fig. 2A). This pattern strongly emphasized cerebellar asymmetries, with a focus on cerebellar lobule VIIIa, 8b, 9 asymmetries in the same direction, alongside ipsilateral shifts in language-related cortical grey matter features including the supramarginal gyrus and contralateral central operculum cortex (Fig. 1B). In addition to exhibiting the largest absolute intraindividual change of brain structure (MBAC), pattern 6 also exhibited the largest

absolute LBAC across all examined asymmetry patterns, suggesting a common motif across the population wherein cerebellar homologues become more left biased with time. The directional trend of asymmetry pattern 6 progression (LBAC) was associated with greater right versus left cortical volume decline. At timepoint 1, interindividual differences in expression in pattern 6 was associated with the second largest number of phenotypes of all examined patterns (126 hits above Bonferroni, 204 above FDR threshold). These associations involved phenotypes across the full breadth of phenotypic domains. Cognitive associations included performance on language-related fluid intelligence questions and trail-making task performance, while mental health associations included medical-doctor diagnosed depression, neuroticism and adverse life events, such as domestic abuse. Pattern 6 was also associated with serum levels of immune cells, including lymphocyte, monocyte, and eosinophil counts.

Taken together, brain asymmetry patterns which exhibited large effect sizes (i.e., large MBACs) did not necessarily also exhibit consistent directionality of change (i.e., LBACs). However, patterns which exhibited large MBACs consistently drew upon distinct and complementary brain locations of left-right divergence. By contrast, the two patterns with the largest LBACs both drew upon cerebellar regional masses: pattern 6 (largest LBAC) emphasizes lobes 8, 9 and crus I and II; asymmetry pattern 16 emphasizes cerebellar lobes 6, 7b and crus II. Pattern 16 emphasizes concurrently cerebellar shifts with white matter asymmetries, including asymmetries in cerebellar and cerebral peduncles, medial lemniscus, and corticospinal tract. Instead, pattern 6 systematically related cerebellar asymmetries to cortical regions rather than white matter tracts.

Large asymmetry changes occur in both directions throughout adulthood

Each asymmetry pattern weighs a set of brain features spanning multiple levels of brain organisation according to their linked deviations from symmetry. Thus, these asymmetry patterns reflect a statistical relationship between brain features observed at the population level. Each individual pattern captures a distinct manifestation of structural brain asymmetry, and together they define the total structural asymmetry observed in the population. We focussed on the 33 statistically defensible patterns that we previously reported to emerge at the population level²⁸. Our present analysis of the longitudinal change in these robust asymmetry patterns revealed common underlying motifs linking brain asymmetry changes within an individual over time. We also confirmed that LBACs and MBACs describe unique aspects of asymmetry changes, as noted by the weak correlation between LBACs and MBACs (mean $|r| 0.04 \pm 0.03$; 1108 / 2145 correlations with pvalues < 0.05; 554/2145 correlations with p-values < 0.05/2145 (Bonferroni correction)) across our UKBB participants (Supplementary Fig. 1C). LBAC and MBACs of the same pattern showed the strongest correlation (mean |r| 0.13 ± 0.08 ; mean $p = 0.051 \pm 0.125$; 28 patterns with p-value < 0.05; 22 patterns with p-values < 0.05/33 (Bonferroni correction)). The complementarity of the separate measures of brain asymmetry change suggests that large absolute asymmetry changes (MBACs) can occur regardless of the direction of change (as captured by LBACs). We also noted that MBACs are weakly coupled with one another ($|r| = 0.12 \pm 0.06$ (mean + std) mean p = 0.02, with maximum |r| 0.45 between MBACS in pattern 2 & 3(p = 6.65e-73)), suggesting that brain asymmetry exhibits appreciable changes in adulthood across the whole brain in multiple distinct ways (Supplementary Fig. 1C). These elements point to structural brain asymmetry as a dynamically shifting property of human brain organisation.

Asymmetry patterns were initially constructed using singular value decomposition to integrate structural brain asymmetries across the brain. Therefore, all asymmetry patterns are by definition linearly independent from one another at the population level²⁸. Yet, we revealed that the longitudinal trajectories of these distinct patterns nevertheless exhibited interdependencies (Supplementary Fig. 1C). The existence of these interrelationships between distinct asymmetry patterns suggests that asymmetry patterns are potentially subject to similar driving factors which result in an observed trend of changes in one asymmetry pattern to be linked to changes in other patterns.

However, the interrelationship between different patterns is not driven by a joint emphasis on the same constituent brain features. For example, two asymmetry patterns which both strongly weigh brain feature A may be expected to exhibit similar overall structural asymmetry change over time as a result of the joint emphasis on brain feature A. However, this phenomenon is not always observed. For example, directional (lateralized) progression over time of pattern 2 and pattern 3 expression (LBACs) exhibited the largest observed absolute correlation across all examined interrelationships (r = -0.66; p = 3.0e-180). Both patterns 2 and 3 implicate planum temporale asymmetry change as a driving contributor to the overall asymmetry pattern. However, both asymmetry patterns call upon the planum temporale such that greater left versus right cortical decline would result in a positive-valued LBACs in both patterns. Yet, positive-valued pattern 3 LBACs were linked to negative-valued pattern 2 LBACs in the same individual. Thus, the relationship between patterns 2 and 3 LBACs is perhaps driven by the concurrent asymmetry shifts in distinct brain features, such as cerebellar lobules VI and VIIb in pattern 2 and the hippocampus and Heschl's gyrus in pattern 3.

Linked brain asymmetry changes also occurred in the absence of overlapping brain features. For example, the second largest absolute correlation between asymmetry pattern changes was the relationship between changes in patterns 3 and 8 (LBACs, r = -0.51, p = 1.0e-96). Pattern 3 draws upon ipsilateral asymmetry changes in the planum

temporale, superior temporal gyrus, Heschl's gyrus, and hippocampus. Pattern 8 draws upon ipsilateral asymmetry changes in inferior and middle temporale gyrus, temporal fusiform cortex, pars triangularis of inferior frontal gyrus alongside contralateral changes in superior temporal gyrus, temporal pole and occipital fusiform gyrus. Of the top 10 brain atlas features describing pattern 3, none are among the top 10 features describing pattern 8. In fact, the planum temporale, which is the single strongest driving feature of pattern 3, is the second smallest contributor to pattern 8 expression (84th out of 85 constituent brain features).

In summary, while asymmetry patterns are linearly independent from one another at the first measurement time point by construction²⁸, we found interdependencies between longitudinal changes of these distinct patterns. This observation suggests potential common underlying motifs governing how brain asymmetry changes within an individual over time. In addition, LBACs and MBACs are largely unrelated from each other, indicating that a double-pronged approach to investigating brain asymmetry change opens a more holistic window onto how hemispheric differences progresse within and across individuals.

Brain asymmetry changes explain total brain volume change better than age and sex

Next, we examined the relationship between total brain volume change, a global measure of brain structure progression, and our measures of asymmetry pattern change. Middle and late adulthood (age 35+) is typically associated with overall brain volume loss, with healthy individuals over age 60 showing steady brain volume losses of > 0.5% per year (Hedman 2012). We used L2-penalised linear models to predict overall brain matter change across different tissue types, given exclusively longitudinal asymmetry pattern information (either LBAC or MBAC). These results were compared against models that only have access to information about age and sex (including common covariates of nonlinear terms: age², age*sex, age²*sex). Age and sex are usually among the strongest obtainable effects in human brain biology in general and in structural brain scans in particular³0-35, and may be meaningfully tied to changes in brain volume³1,36

Importantly, asymmetry-pattern models (LBACs, MBACs) performed better than analogous age-sex models in explaining total brain volume progression between participants (Supp Fig. 2). Yet, when considering overall brain volume, rather than its change, asymmetry-pattern models (LBACs, MBACs) performed worse than analogous age-sex models (Supplementary Fig. 3). Better performance in explaining total brain volume change when considering asymmetry pattern progression instead of age and sex persisted across different types of brain tissues – grey matter only, white matter only, or combined grey and white matter— examined. Models with information about either LBACs or MBACs are consistently able to track changes in total brain volume across all types of brain mass assessed (Supplementary Fig. 2).

By contrast, age-sex models performed more poorly in explaining total brain volume change than models with access to baseline hemispheric asymmetry information only (Supplementary Fig. 2). That is, the structural asymmetry of a brain at a given timepoint is more strongly tied to the future changes in overall brain volume, that individuals undergo over the course of years, than age or sex. The ability of lateralized brain asymmetry changes to explain gross brain volume change is most apparent when assessing change in total white matter volume. Notably, our asymmetry patterns do not directly contain information about white matter volume, but rather dMRI-derived measures of white matter integrity.

If overall brain structural change in general did not progress in an asymmetric manner, we would expect that overall brain change would not be reflected by brain asymmetry changes. We reason that, if changes in brain structure – either overall growth or overall decline – occur at an equal rate in both hemispheres, individual divergences in the relative rate of decline or growth between hemispheres, as captured by LBACs and MBACs, would not provide additional information on overall structural brain change. On the other hand, if brain changes occurred at a different pace in each homologue, measures capturing the relative difference in rate of change across hemispheres, such as LBACs and MBACs, would be able to capture total structural brain change, as encountered in our analyses.

In particular, greater rates of total white matter volume loss are associated with smaller MBACs in patterns 2 (associated with planum temporale asymmetry) and smaller MBACs in pattern 10 (associated with supramarginal gyrus asymmetries). Change in asymmetry pattern 1 expression (LBAC) associated with more prominent right-frontal leftoccipital brain torque at the second timepoint was associated with greater rates of total white matter volume loss. Knowledge of brain asymmetry in isolation of knowledge of its longitudinal trajectory was as informative as knowing age and sex in developing a model of longitudinal change of gross brain volume. That is, the structural asymmetry of a brain at a given time point is tied with the future changes in brain volume that individuals were to undergo over the course of years. Overall, changes in total brain volume can be viewed as a reflection of added-up component effects from longitudinal changes in structural brain asymmetry of spatially distributed brain features. These findings attest to the biological meaningfulness and strength of effects of our examined longitudinal asymmetry pattern measures.

Sex and age tie into how much, but not how, brain asymmetry is progressing

Many cognitive processes, including those sensitive to sex- or agerelated differences, are tied to structural asymmetries. Biological sex plays a salient role in cognitive processes spanning from language, to viso-spatial reasoning, to social reasoning^{33,37,38}. We next explored the role of sex and age in longitudinal changes in brain asymmetry, starting with how asymmetry patterns reconfigure over time (LBACs). Among our collection of examined asymmetry patterns, the longitudinal progression in brain asymmetry was most starkly different between males and females in asymmetry pattern 21 (t(1423) = -3.32, p = 0.0009, Cohen's d = -0.176), followed by pattern 17 (T(1423) = 1.99, p = 0.046, Cohen's d = 0.106), which tracks ipsilateral cerebellar lobule VIIIb, parietal operculum cortex and inferior temporal gyrus asymmetries (Fig. 1B).

Age at baseline exhibited large effects in directional progression of brain asymmetry across multiple patterns (Supplementary Fig. 1D), including pattern 20 (T(685) = 2.88, p = 0.0041, Cohen's d = 0.219), pattern 6 (T(685) = 2.05, p = 0.041, Cohen's d = 0.156), and pattern 16 (T(685) = 1.70, p = 0.090, Cohen's d = -0.130). Pattern 21 was the most dissimilar between the sexes (T (1423) = -3.32, p = 0.0009, Cohen's d = -0.176) yet longitudinal progression of this asymmetry motif appeared similar in relatively younger and relatively older individuals (T (685) = 0.06, p = 0.950, Cohen's d = 0.005). Asymmetry pattern 21 combines ipsilateral asymmetries grey matter regions, including the middle frontal gyrus, amygdala, and paracingulate gyrus, with asymmetries in contralateral white matter tracts, including posterior corona radiata, medial lemniscus, and corticospinal tract. The Cohen's d sex contrast indicated that male participants, on average, exhibited stronger asymmetry shifts corresponding to a left cortex undergoing larger longitudinal volume declines than the right cortex, compared to females. The result of the Cohen's d analysis indicates a relative separation between the male and female UKBB participants, but does not directly convey the mean asymmetry change in either group. When examining the mean LBAC change in males and females, respectively, we found that the mean pattern 21 LBAC in males is positive (indicating a left cortex shrinking faster than the right cortex), whereas the mean LBAC in females is negative (indicating the right cortex shrinking faster than the left cortex). That is, the mean female exhibited pattern 21 asymmetry shifts in the opposite direction as the mean male. The number of males (n = 695) and females (n = 730) is relatively balanced in the cohort, and males exhibiting slightly larger amounts of changes relative to females (T = 0.60, p = 0.547, Cohen's d = -0.042). The combined effect of similar magnitude of asymmetry changes (MBACs) across sexes but in opposite directions may contribute to the observation of an across-population mean LBAC consistent with zero in pattern 21 (Fig. 1A). Nevertheless, this motif of sex-dependent longitudinal progression of asymmetry seems limited to the sex-dependent asymmetry pattern 21. Only three other asymmetry patterns (patterns 4, 14, and 15) exhibited LBACs in opposite directions in males and females, with absolute sex-contrast Cohen's d ranging from 0.034 (pattern 4) to 0.102 (pattern 14) $(T_s(1423) = \{-0.64, 1.93, -1.51\}$, $p = \{0.52, 0.053, 0.130\}$, Cohen's $d = \{-0.34, 0.10, -0.08\}$ for patterns 4, 14, 15, respectively). Overall, we found that asymmetry pattern progressions in general occur in the same direction (LBAC in the same direction) between sexes across most examined patterns.

Sex-specific trajectories in asymmetry pattern changes cannot be entirely attributed to sex-differences in initial asymmetry pattern expression at baseline. Among our catalogue of 33 examined asymmetry patterns, 25 patterns exhibited significant sex-related divergences in expression at time point 1, that is, without considering longitudinal brain change²⁸. Here now, the Cohen's d analysis examining the sex-related divergences in asymmetry pattern changes (LBACs) of these 25 patterns yielded absolute Cohen's d ranging from 0.021 (pattern 13, T(1423) = -0.39, p = 0.70) to 0.176 (pattern 21, t(1423) = -3.32, p = 0.0009). Asymmetry pattern 6 exhibited the largest sex divergence in pattern expression at baseline²⁸, yet revealed small sex differences in the longitudinal progression of pattern expression (Cohen's d = -0.024, t(1423) = -0.45, p = 0.65; Fig. 2B). Overall, we find modest differences in the changes in hemispheric balance in males and in females even in asymmetry patterns where baseline asymmetry was significantly different between the sexes.

From the alternative perspective of asymmetry magnitude change (MBACs), our results revealed a consistent trend for males to show larger absolute asymmetry changes than females. MBACs in males exceeded MBACs in females in 29 out of 33 asymmetry patterns. Overall, we find that particular motifs of hemispheric asymmetry appear particularly sensitive to biological sex, providing hints that demographic characteristics may lead to specific asymmetry changes. Asymmetry pattern 6 showed the largest asymmetry magnitude difference in males compared to females (Cohen's d = -0.240; t(1423) = -4.5, p = 6.6e-6), indicating that the rate of asymmetry changes in males exceeds that in females. Of the 4 asymmetry patterns where change magnitude in females exceeded that of males (patterns 20, 23, 27, 32), Cohen's d effect sizes were modest, ranging from 0.032 to 0.050, and none were significant (all p-values > 0.05). By contrast, the trend for males to exhibit larger gross amounts of asymmetry change compared to females extended across a greater number of asymmetry patterns, and exhibited larger effect sizes (Supplementary Fig. 1A). Taken together, the larger effect size of sex divergences in MBACs as compared to LBACs indicates sex impacts how much brain asymmetry changes more strongly than it impacts how brain asymmetry changes. This could be potential reason for why larger brain asymmetries are observed in males rather than females.

Next, to investigate the role of age in the continuous progression of whole-brain asymmetries within individuals, the cohort was partitioned by age brackets, and the longitudinal brain asymmetry change was contrasted between the 25% oldest participants at baseline (age \ge 69 years old; n = 342) and the 25% youngest participants at baseline (age \le 58 years old; n = 345). The effect sizes separating the LBACs of the relatively older and relatively younger participants were modest (mean absolute effect size $d = 0.0649 \pm 0.0504$ across 33 patterns). Asymmetry pattern 6 displayed the largest LBACs across the cohort (Fig. 1B) alongside small sex effects (sex Cohen's d = 0.024,t(1423) = -0.45, p = 0.65; Fig. 1C) but the second largest absolute effect size of

relative age (Cohen's d = 0.156, t(685) = 2.0, p = 0.041). Relatively older individuals displayed larger shifts in asymmetries of brain features, including cerebellum lobules 8 and 9 alongside lingual gyrus and posterior supramarginal gyrus, compared to relatively younger individuals. Examining the absolute amount of change in relatively older compared to younger adults revealed a consistent motif of faster rates of brain asymmetry change characterising relatively older individuals (Cohen's d < 0 in 32 examined patterns, associated with larger MBACs in older adults). Age-related effect sizes in MBACs (mean absolute effect size d = 0.176 \pm 0.079 across 33 pattern MBACs) consistently exceeded effect sizes in LBACs. Age was associated with larger effect sizes in comparison to sex-related variation across our analyses.

Finally, we conducted a subanalysis to assess the contribution of handedness on structural changes in brain asymmetry. Group differences between self-reported right-handed (n=1271) and left-handed (n=131) individuals revealed a trend across patterns for left-handedness to be associated with larger amounts of asymmetry change (MBACs) was observed (right – left Cohen's d<0 in 24 patterns). On the whole, handedness-related effect sizes in MBACs (mean absolute effect size d=0.083±0.064) were larger than handedness-related effect sizes in LBACs (mean absolute effect size d=0.064±0.042). Handedness-related LBACs and MBACs did not exceed the largest (absolute) effect size between the sexes (Supplementary Fig. 1E).

Overall, we found that both age and sex are meaningfully tied to within-subject trajectories of global brain asymmetry (both LBACs and MBACs), with age being the more explanatory factor for both measures of global brain asymmetry progression. Both age and sex are tied to how much brain asymmetry changes (MBAC) more strongly than these two factors are tied to how brain asymmetry changes (LBAC).

Transitioning into a new phase of life shows sequalae in brain asymmetry reconfigurations

Investigations into longitudinal changes in brain structure to date have repeatedly highlighted the role of regular training and skills development as precursors to plastic brain adaptations, as measurable by MRI technology, even over the course of weeks (cf. Introduction). Here, 2-3 years elapsed between consecutive structural brain scans, over which time larger changes in lifestyle and behaviour may potentially occur. Because structural brain scans measurements, unlike functional brain scans, are not influenced by in-scanner tasks or activities, it has been argued that the resultant neuroanatomical measures are particularly well suited to capturing brain correlates of lifestyle factors measured in ecologically valid (non-scanner) scenarios9. In this spirit, we turned to the onset of retirement (a lifestyle factor) to carry out a naturalistic study, or quasi-experiment, on how a major transition from one life phase to another may ignite plastic structural brain changes; which would be consistently identifiable across several hundred individuals.

Leaving the workforce for retirement marks an important inflection point in individuals' lives. This transition has wide-ranging repercussions on the social environment, sense of purpose, and daily environmental exposures. Therefore, we confronted retirement as a prime target to organically investigate how major life events may coincide with reconfigurations of structural brain asymmetry. We considered (i) individuals in full-time employment at both imaging visits (n = 870 UKBB biobank participants), (ii) individuals in retirement at both imaging visits (n = 308), and (iii) individuals who transitioned between these two life phases in the years between imaging visits (n = 121); henceforth retiring). To analyze how such distinct demographic statuses relate to brain asymmetry change, we computed Cohen's d group differences in three separate contrasts of employment status pairs. We found that effect size strengths across all employment contrasts consistently exceeded the largest effect size of the most sex-dependent pattern, suggesting that tangible lifestyle factors may have more prominent relationships with brain asymmetry reconfigurations than more traditionally studied "covariate" factors such as sex. Our collective findings (LBAC effects > MBAC effects) suggest that within-subject brain changes depending on employment status may be tied to preferred direction, left to right or right towards left hemisphere, rather than magnitude, of hemispheric asymmetry shifts

Retirement emerged as a salient feature describing rearrangements in several of our asymmetry patterns. Six separate asymmetry patterns exhibited absolute Cohen's d > 0.175, the level of the strongest sex differences in our study (cf. above), in at least one contrast (Fig. 2B, C). In 3 of the 6 most employment-sensitive patterns, the most relevant employment contrast occurred when comparing brain morphology changes in individuals in full-time employment at both time points to those in full-time retirement at both time points. These asymmetry patterns drew upon largely distinct local shifts. Fulltime employment versus retirement distinguished longitudinal shifts in asymmetry pattern 25 (employed - retired Cohen's d=-0.220, t(1176) = -3.31, p = 0.00096; Fig. 2B), which drew upon asymmetries in white matter fibres including ipsilateral shifts in cerebral peduncle, posterior internal capsule and superior corona radiata; and also implicated asymmetries in ipsilateral pallidum and contralateral ventral striatum (Fig. 1B). In addition, the retirement versus employment contrast flagged pattern 15 (employed – retired Cohen's d = -0.206; t(1176) = -3.11, p = .0019; Fig. 2B) and pattern 7 (employed – retired Cohen's d = -0.197; t(1176) = -2.97, p = .0030; Fig. 2B). Pattern 15 drew upon structural asymmetry changes particularly in cortical regions, including ipsilateral angular gyrus, subcallosal cortex and contralateral postcentral gyrus; as well as crus I of the cerebellum and ventral striatum. Overall, embarking on new ways of life (full-time employment versus long-term retirement) reverberates in longitudinal structural brain changes across spatially distributed brain features in an asymmetric manner.

We next shift focus away from the contrast between static work environments (employed against retirement) towards the transition into retirement itself in our UK Biobank participants. We observed the largest retirement-related effect size across all contrasts (33 patterns x 3 retirement contrasts) emerged in pattern 19's change directions (LBACs) when contrasting retiring individuals (whose retirement occurred in the 2-3 year interval between consecutive imaging visits) versus retired individuals (whose retirement occurred prior to the first imaging visit). Pattern 19 draws upon asymmetries in ipsilateral temporal occipital fusiform gyrus, middle frontal gyrus and anterior parahippocampal gyrus, alongside concurrent contralateral shifts in tapetum, and posterior thalamic radiation fibre tracts (Fig. 1B). Pattern 19 LBACs in retiring individual appeared distinct from those in both retired individuals (retiring – retired Cohen's d = 0.292; t(427) = 2.73; p = .0066; Fig. 2C) and employed individuals (employed – retiring Cohen's d = -0.210, t(989) = 2.19; p = .029; Fig. 2C). By contrast, the longitudinal trajectories of pattern 19 expression appeared more similar in retired versus employed individuals (employed - retired Cohen's d = 0.100; t(1176) = 1.51; p = .13; Fig. 1A). Taken together, the three group contrasts suggested that the onset of retirement coincided with longitudinal reconfigurations of brain asymmetry in a distinct way from reconfigurations observed in either type of stable employment environment. Beyond pattern 19, we found that the transition to retirement (contrasting full-time employment) yielded effects in asymmetry patterns 9 (employed-retiring Cohen's d = 0.198; t(989) = 2.04; p = .42; Fig. 2C), which highlights asymmetries in cerebellum, fusiform cortex, and supramarginal gyrus, as well as pattern 14 (employed – retiring Cohen's d = 0.181; t(989) = 1.86; p = .063; Fig. 2C) with asymmetry effects in frontal pole and medial lemniscus. The collective findings suggest that the very act of retirement - a major life transformation - tended to co-occur with dedicated left-right hemisphere shifts distributed across the whole brain.

Subsequently, we compared magnitude against direction properties in these progressions of hemispheric reorganisations. We consistently observed that direction effects (LBACs) were larger than magnitude effects in brain asymmetry change (MBACs) across retirement groups. In contrast to sex and age effects (cf. above), retirement resonated more with how asymmetry changes rather than how much asymmetry patterns change. Nevertheless, our MBAC analyses shed light on how the various employment states influence brain asymmetry change. Consistently across patterns, the absolute rate of brain asymmetry change (MBAC) was faster in individuals who are retired as compared to individuals who are employed (employed - retired Cohen's d contrast is < 0 in 28 out of 33 patterns; Supplementary Fig. 1A). Individuals who were retired also displayed faster absolute rates of asymmetry change than individuals who were retiring (retiring – retired Cohen's d < 0 across 25 patterns; Supplementary Fig. 1B). These two findings suggest that the greatest amount of asymmetry change across all three employment groups (employed, retired and retiring) occurred within the retired group (for more details also see Supplementary Fig. 1).

Taken together, the act of retirement marks an incisive turning point in one's life, which may also help neuroscientists see deeper into longitudinal progression of whole-brain structural asymmetry. We found retirement – and its contemporaneous revision in living environment – on the whole to be especially closely tied into how (rather than how much) asymmetry patterns progressed. Different life stages impacted distributed sets of local asymmetries in distinct ways. Notably, retirement-related asymmetry effect sizes exceeded those of sex effects, suggesting that lifestyle may explain more variation in within-subject asymmetry progression than more commonly studied demographic factors.

Day-to-day lifestyle and cognitive performance are reflected in brain asymmetry changes

Next, we extended our investigation of the real-world relevance of the observed asymmetry pattern trajectories beyond employment status change, towards a variety of other candidate changes in behaviour and environment that potentially evoke neural processes that contribute to plastic remodelling. To gain a phenome-wide synopsis of how changes in various lifestyle indicators may resonate in the withinindividual changes of whole-brain asymmetry motifs, we conducted L2 penalised linear regression analyzes predicting asymmetry pattern changes based on a rich array of behavioural/lifestyle phenotypes and phenotype changes (cf. methods). Our phenotypes spanned a total of 11 domains as measured at the initial UKBB visit, ranging from mental health to cardiac measures, to blood assay results to early life factors. For brevity, we refer to this collection of phenotypes as lifestyle and behavioural factors. Phenotype changes captured differences in questionnaire responses / physical assessment as assessed at each imaging visit. Within each domain, a model estimating brain asymmetry change was constructed integrating one domain of either baseline or change in phenotypes alongside to demographic indicators (age, sex, age-sex covariates) and time between visits. To confirm the added value of considering lifestyle variables from these demographic indicators in assessing brain asymmetry change, we compared against base models containing only age, sex, age-sex covariates, and time between visits with no additional lifestyle phenotypes (cf. methods). In so doing, we systematically charted how a palette of life domains reverberate in longitudinal brain asymmetry changes.

As a recurring tendency, changes in asymmetry patterns were explained by baseline mental health self-report markers, cognitive performance, and various lifestyle indicators (Fig. 3a). This trifecta persisted across measured kinds of brain asymmetry change (MBACs and LBACs) and across examined patterns (Supplementary Fig. 5). Correcting for handedness did not appreciably change the discovered asymmetry-trait relations (Pearson's r = 0.9986, p << 0.05 for adjusted

R² scores with and without handedness correction). In addition, specific asymmetry patterns were characterised by distinct sets of lifestyle and behavioural indicators. For example, we previously discovered a relationship between LBACs in asymmetry pattern 19 and transitioning into retirement. This relationship was recovered in the current analysis linking pattern 19 LBACs, where transition to retirement was found to be meaningfully related to longitudinal progression in asymmetry pattern 19. Adding to the relationship between pattern 19 and retirement (cf. above), its change directions (LBACs) were related to both baseline and changes in measures of socioeconomic status, including educational attainment, local employment and crime scores. In contrast, asymmetry pattern 16, which showed small retirement-related effect sizes across all contrasts, was linked to baseline measures of socioeconomic status only, namely household income and local greenspace and pollution measures. Asymmetry pattern 16 was not linked to transitioning into retirement, but was linked to changes in life stressors, such as the development of illnesses or death in close family members. Distinct lifestyle factors hence related to separate brain asymmetry progression.

Our next aim was to further probe and delineate the lifestyle motifs which drove the observed brain asymmetry change --- behaviour relationships uncovered in a more principled manner. To this end, we applied principal component analysis on the coefficients of the collection of derived behaviour-brain models (L2-penalised linear regression models), one estimated model for each target phenotype in the phenome repertoire. Across asymmetry patterns, living in a rural versus urban environment tracked MBACs to a stronger extent than LBACs (Supplementary Fig. 5). MBACs were additionally related to familial instances of Alzheimer's and related dementias; which were not as relevant for LBACs. Social home environment, such as living with relatives, was more relevant for how brain asymmetry progresses (LBACs) than how much (MBACs). Performance on specific cognitive tasks aimed at assessing fluid intelligence was relevant for describing both LBACs and MBACs. Mental health phenotypes, and in particular mental health diagnoses, were reflective of LBACs and MBACs. Age and sex did not reflect the longitudinal progression of brain asymmetry as strongly as these specific domains of lifestyle and behaviour.

As a complementary assessment of the interplay between changes in lifestyle indicators and changes in whole-brain asymmetry patterns, we conducted a separate assessment examining how brain changes relate to lifestyle changes, as opposed to the reversed situation described above. More specifically, we conducted L2 penalised linear regression models predicting change in behavioural phenotypes on the basis of asymmetry pattern changes (both LBACs and MBACs) and demographic and technical features (time between visits, age, sex, and their covariates). The results of these analyses were compared to the explanatory power obtained when only demographic and technical features were included in regression models.

We observed a rich palette of links of brain asymmetry changes to socioeconomic status indicators, cognitive functioning, and health. Socioeconomic status indicators, such as change in household income and home heating type, were linked to asymmetry pattern change (Fig. 3B). For example, directional change in asymmetry pattern 6 (LBAC) was the strongest regressor in evaluating change in total household income. Varied performance on fluid-intelligence questions across imaging visits was linked to brain asymmetry changes. In particular, questions which involved language proficiency, such as word or concept interpolation. Finally, altered health status of family members revealed links to changes in brain asymmetry. These findings remained virtually identical after correcting asymmetry change for handedness prior to analysis (Pearson's r = 0.9996, $p \ll 0.05$ for R² scores with and without handedness correction). Overall, our findings point to a complex interplay between various aspects of different life sectors and the progression of brain asymmetry patterns.

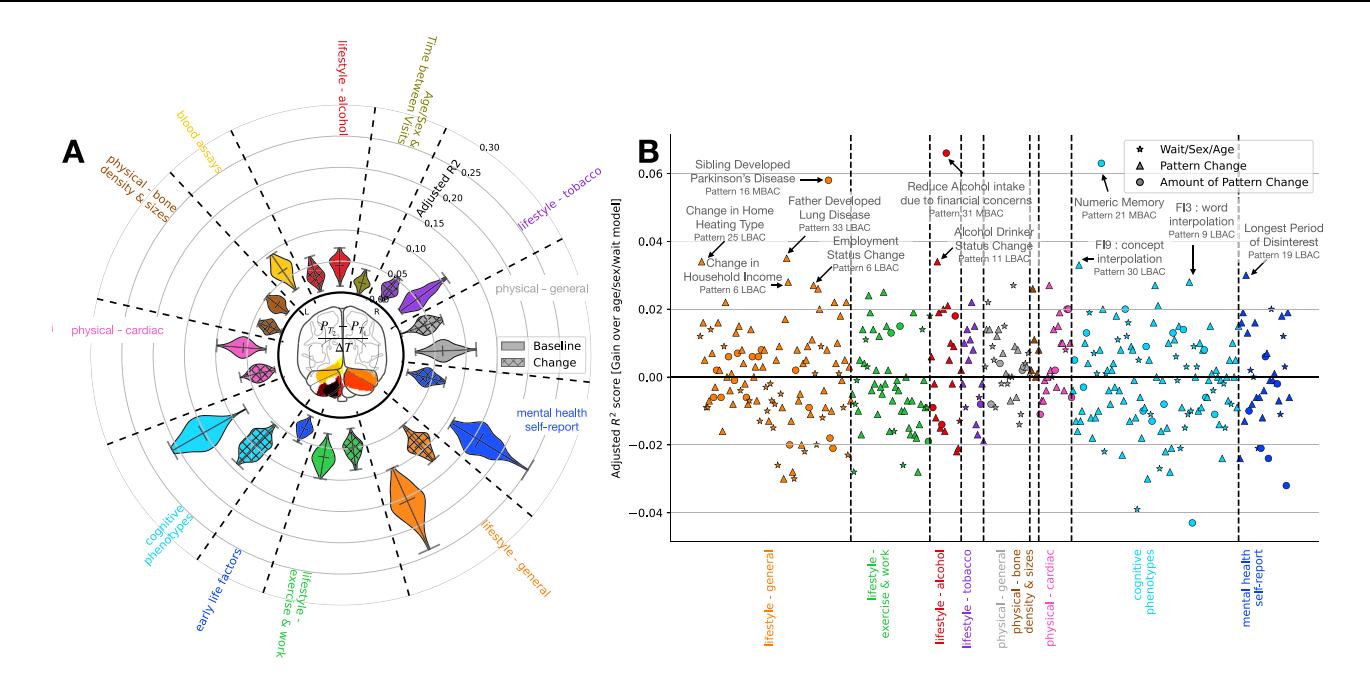


Fig. 3 | Changes in lifestyle and cognition are reflected in changes in structural brain asymmetry. A Specific behavioural domains capture the longitudinal progression of brain asymmetry. Coefficient of determination (R²) of L2 penalised linear regression models across 100 bootstrap replicates predicting pattern 6 longitudinal asymmetry change (LBAC) on the basis of behavioural phenotypes within a given domain. All models additionally contained sex, age at first imaging visit, and time between visits information. R² scores were adjusted for the number of parameters in the models. Mean adjusted R² scores are indicated. Phenotype changes represent the difference in response variables between the first and second imaging visits, and do not contain information about baseline response. Cerebellar contributions to pattern 6 are showcased in the centre of the graph. Ipsilateral cerebellar lobule VIIIa, 8b, 9 shifts alongside contralateral cerebellum crus I and II shifts characterise asymmetry pattern 6. **B** Whole-brain asymmetry

pattern changes reflect changes in lifestyle and behaviour. Coefficient of determination (R²) gain derived from including LBAC and magnitude of asymmetry change (MBAC) information in L2 penalised linear regression models predicting a behavioural phenotype on the basis of non-brain variables as well as brain asymmetry changes. Baseline comparison models contained only information about age, sex, and time between visits. R² scores were adjusted for the number of parameters in the models. A separate regression model was constructed for each phenotype. The shape of points represents the largest absolute coefficient contributing to the behavioural prediction, categorised according to membership to LBAC (triangle), MBAC (circle) or non-brain variables (age, sex, time between visits; star). Measures of socioeconomic status, including change in household income and employment status, feature among phenotypic changes linked to structural brain asymmetry change. Source data are provided as a Source Data file.

Measures of brain asymmetry change relate to diagnoses from health records

Motivated by cues from self-report health measures (cf. last section), we next capitalised on diagnoses from medical doctors in the linked electronic health record data of UK Biobank participants. To this end, we condensed a total of 4448 ICD codes (both ICD9 and ICD 10) in the UK Biobank imaging cohort into 174 composite disease clusters (cf. "Methods") which combine linked diagnoses. We then conducted a medical diagnosis-wide association study (MeDiWAS) linking brain asymmetry changes to clusters of physician-certified disease spanning 17 broad disease categories, ranging from congenital diseases to respiratory or digestive illnesses to neoplasms.

We thus identified physician-diagnosed mental health disorders to be associated with within-individual changes in brain asymmetry across both methods of quantifying brain asymmetry changes (LBACs and MBACs). In particular, asymmetry pattern 12 LBACs (Pearson's r = 0.105; $p_{uncorrected} = 6.3e-5$) and pattern 13 MBACs (Pearson's r = 0.101; $p_{uncorrected} = 1.3e-4$) were associated with a disease cluster (PLS-MENT-1) encapsulating depression and related diagnoses (major depressive disorder, suicide attempts and suicidal ideation; Fig. 4). These two brain asymmetry measures were weakly correlated to each other (Pearson's r = -0.011, Supplementary Fig. 1C), and highlighted asymmetries in separate areas of the brain. Pattern 12 highlights concurrent asymmetry shifts in ipsilateral lingual and anterior cingulate gyrus and contralateral superior frontal gyrus. Pattern 13 emphasized concurrent asymmetry shifts in the postcentral gyrus, posterior middle temporal gyrus, and anterior supramarginal gyrus alongside contralateral shifts in asymmetry of the angular gyrus and parietal

operculum cortex. Pattern 12 LBACs (Pearson's r = 0.116; $p_{uncorrected}$ = 1.2e-5), but not pattern 13 MBACs (Pearson's r = 0.084; $p_{uncorrected}$ = .001), were associated with a disease cluster (PCA-MENT-3) implicating physician-diagnosed anxiety disorder diagnoses. Our previously noted relationship between self-reported mental health indicators and brain asymmetry changes (cf. previous section) was reflected by here-discovered associations between specific longitudinal whole-brain asymmetry changes and physician-diagnosed clinical mental health and psychological disorders.

Several disease categories outside of mental health emerged as relevant in our analysis. For example, the magnitude of changes in pattern 8, which highlights asymmetries in the temporal gyrus with particular emphasis on inferior temporal gyrus and temporal fusiform cortex, was linked to a disease cluster (PLS-NEUR-3) emphasizing sleep disorders, including insomnia (F51.X, G47.X, 307.4), and sleep apnoea (G47.3) (Pearson's r = 0.094; $p_{uncorrected} = 4.1e-4$; Fig. 4). A separate category of diseases, dermatological disorders, emerged as significantly associated with measures of brain asymmetry change. Clusters within the dermatological disorder category were linked to both MBACs and LBACs in circumscribed brain asymmetry patterns. In particular, a cluster of dermatological conditions (PCA-DERM-4) including ichthyosis, scleroderma, actinic keratosis, and scarring conditions including keloids was significantly associated to changes in asymmetry patterns 27 (LBAC (Pearson's r = -0.122; $p_{uncorrected} = 3.8e$ -6) and MBAC(Pearson's r = 0.123; $p_{uncorrected} = 3.3e-6$)) and 31 (MBAC only (Pearson's r = 0.132; $p_{uncorrected} = 6.0e-7$)) (Fig. 4). Asymmetry pattern 27 implicates asymmetry of the temporooccipital part of inferior temporal gyrus alongside ipsilateral asymmetry of posterior

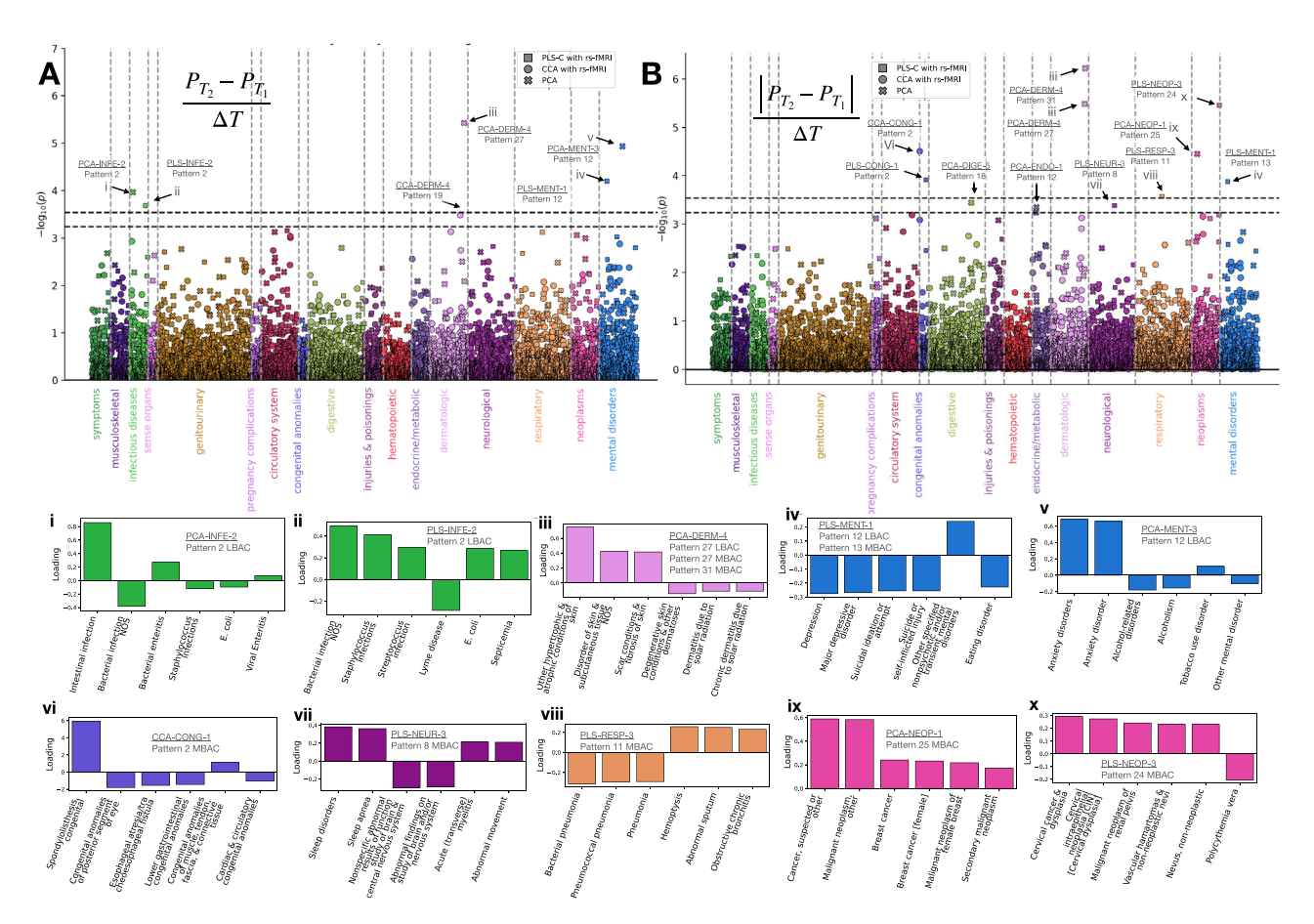


Fig. 4 | **Diagnoses from physicians relate to measures of brain asymmetry change.** Manhattan plots relate (**A**) longitudinal brain asymmetry changes (LBACs) and (**B**) magnitude of brain asymmetry changes (MBACs) across the population to 174 composite disease clusters spread across 17 domains. For each composite disease cluster, two-sided Pearson correlation coefficients are shown in units on a logarithmic scale of the associated *P*-value. Results from all 33 distinct asymmetry patterns are showcased. Horizontal lines indicate the significance thresholds at FDR labelled FDR, Bonferroni correction (0.05/174) labelled BON, with 5 and 6(LBAC) or 8 and 12 (MBAC) phenotypes passing each respective threshold. Composite disease clusters were constructed either by (i) PCA on 1662 medical diagnosis phecodes from the full UKBB cohort (-500,000 individuals) (crosses) (ii) CCA on 1447 medical diagnosis phecodes from the brain imaging UKBB cohort (-40,000 individuals) and resting state fMRI (circles), or (iii) PLS-C on 1447 medical diagnosis phecodes from the brain imaging UKBB cohort (-40,000 individuals) and resting

state fMRI (squares). Inlaid barplots showcase the 6 largest absolute medical diagnoses phecodes which contribute to a composite disease cluster. Text within inlaid graphs indicates the composite disease cluster name and which asymmetry pattern change(s) it was significantly correlated to. Composite disease clusters are named in the format METHOD-DOMAIN-#, where METHOD is a 3-character code for the data compression technique (PCA, CCA, or PLS-C); DOMAIN is a 4 letter code indicating the first 4 characters of the associate disease domain (for example, NEOP indicates neoplasms), and the number indicates the latent-factor component for the corresponding method (for example, PCA components 1 or 2). In short, brain asymmetry changes are consistently related to common physician-diagnosed mental health disorders, including depression, suicidality and anxiety, substance use and sleep disorders. NOS not otherwise specified; CIN Cervical intraepithelial neoplasia. Source data are provided as a Source Data file.

cingulate gyrus and contralateral asymmetry in superior parietal lobule. Asymmetry pattern 31 meanwhile implicates asymmetry in white matter tracts involved in linking areas of the limbic system, including uncinate fasciculus and cingulum cingulate gyrus. Skin scarring, which we here linked to circumscribed changes in wholebrain asymmetry patterns, is known to result in poorer emotional wellbeing and quality of life³⁹, while access to dermatological care more broadly have been linked to socioeconomic strata⁴⁰.

Certain further disease categories were tightly linked to changes in particular asymmetry patterns. Asymmetry pattern 2, which links asymmetries in brain features including planum temporale, cerebral peduncle, corticospinal tract, and specific cerebellar lobules including lobules VI, VIIb, and VIIIa, was specifically associated with infectious diseases, with a particular emphasis on intestinal and bacterial infections, including staphococcus, streptococcus and septicemia (Fig. 4). There is a growing body of experimental animal model studies that link the gastrointestinal tract and its microbiome to the brain and its function (for reviews see^{41–44}. Notably, specific alterations to

the intestinal microbiota of mice, either through administration of antimicrobials or microbiotic transplantation, lead to changes in both behaviour and expression of brain-derived neurotrophic factor, a key neuronal growth factor, within the brain. These changes were independent of autonomic nervous system, gastrointestinal-specific neurotransmitters, or inflammation⁴⁵. Similar research in humans investigating the gut-brain axis is still relatively scarce in comparison to research focused on animal models⁴². In the analysis relating longitudinal changes in brain asymmetry to the aspects of behaviour which may track them (cf. indeed, Fig. 3A), LBACs in asymmetry pattern 2 were related to multiple measures of socioeconomic status, including homeownership status, educational qualifications (NVQ or HND or HNC or equivalent) and taking adult education courses.

In mice, specific alterations to the intestinal microbiota, either through administration of antimicrobials or microbiotic transplantation, lead to changes in behaviour and, notably, to brain-derived neurotrophic factor, a key neuronal growth factor, expression in the brain. These changes were independent of autonomic nervous system, gastrointestinal-specific neurotransmitters, or inflammation⁴⁵.

Overall, we found that changes in the relative hemispheric balance of spatially distributed sets of brain regions show associations with several clusters of physician-assigned medical diagnoses. These MeDiWAS association range from highly specific relations between particular asymmetry patterns and particular disease categories to broader associations between brain asymmetry changes in general and physician-diagnosed disease clusters, particularly in the domains of mental health disorders, sleep disorders, and dermatological conditions.

Discussion

The acquisition of new skills (e.g., learning a new language¹⁷, how to juggle^{3,4} or development of existing ones (e.g., learning new words in a language you already know¹², strengthening empathy skills¹⁵) have been shown to induce structural changes in the adult brain, even across short time spans of hours or weeks in mostly small boutique datasets. Extending our outlook, we here examined brain-global changes in the structural distribution of the brain at a large breadth (population scale), depth (extensive phenotyping) and range (over the course of years). Across our quantitative analyses, our central finding is that brain asymmetry is not static over time across neuroanatomical brain-wide features covering cerebellum, cortex, subcortex, and major white matter tracts. Rather, our collective findings attest to specific longitudinal changes in principled patterns of structural brain asymmetry coherently track hundreds of markers across lifestyle domains. Complementing this finding, we further revealed that structural asymmetry changes are tied into specified disease clusters of physician-diagnosed illnesses (ICD9/10 codes), including clusters encapsulating mental health disorders, like depression and anxiety, and sleep disorders. Taken together, our population-scale findings establish an intimate link between life events and plastic adaptations of brain asymmetry in humans.

One or several of the following recurring characteristics mark previously published brain asymmetry research in the neurosciences: (i) small participant sample size, (ii) cross-sectional study design, (iii) severely limited repertoire of available phenotype measurements, (iv) a focus of quantitative analysis and substantative interpretation on each homologous region pair, separately from all the respective other regions, or v) only considering a single kind of brain measurement modality at once. Until recently, neuroscientific endeavours have on average been conducted on cohorts of dozens of people^{46,47}. Within the field of research on hemispheric asymmetry, there exist only a handful of studies examining cohorts over 1000 individuals^{28,48-51}. Of these large sample size studies, all are limited to cross-sectional cohorts and study designs. Yet, longitudinal changes have been demonstrated to reveal stronger effects than those found in many cross-sectional analyses⁷. Here, to overcome several limitations of this field, we conducted a large-scale (n > 1000) longitudinal study examining structural brain asymmetry. It revealed progression of relative hemispheric structural balances which pervade all examined levels of brain organisation - cortex, subcortex, cerebellum and whitematter fiber bundles. Comprehensive reviews on brain research have also noted a tendency to examine one phenotype of interest in isolation of others⁵²; here, we systematically assessed hundreds of tangible behaviours and lifestyle factors, as well as changes along these phenome-wide dimensions. Examinations of structural asymmetry have often focused on either the cortical shell or subcortical structures, while neglecting cerebellar asymmetry⁴⁸⁻⁵¹. Here, we concurrently considered brain asymmetry across cerebellar, cortical, subcortical, and white matter structures. By overcoming this set of shortcomings, our present study was able to reveal complex, multifaceted dynamics of whole-brain structural brain asymmetry change manifesting over the course of years. Asymmetry pattern changes co-occurred across the population in ways defying simple explanations concentrated on a single anatomical region alone.

Our collection of findings advocate that asymmetry change itself is biologically relevant. Despite a paucity of longitudinal research explicitly targeting hemispheric brain asymmetry change, existing longitudinal studies which focus on regional changes across the brain repeatedly link hemispherically unbalanced changes in brain structure to behaviours spanning social awareness¹⁵, visuospatial awareness^{3,4}, and language¹⁷. Here, we found distributed structural asymmetry change to largely tie into markers of mental health, cognitive abilities, cognitive change, and environmental factors. One's relationship with one's inner social circle is amongst the most important social relationships for one's psychological and physical well-being^{53,54}. Time since last contact is strongly tied to emotional closeness, particularly for kin relationships⁵⁵. Individuals within a shared household may thus represent one's strongest emotional connections as well as most frequently contacted individuals. Our results repeatedly highlighted a relationship between longitudinal progression of brain asymmetry and household composition across patterns. Household composition and size were consistently more strongly related to how brain asymmetry changes (LBAC) than to how much asymmetry changes (MBAC). Frequency of family/friends visit was more strongly linked to amount of brain asymmetry changes (MBAC) rather than directional change (LBAC). Social interactions, and lack thereof, have previously been linked to Alzheimer's disease and related dementia⁵⁶⁻⁵⁸. The link charted herein between social markers and brain asymmetry may thus illuminate one putative factor in the relationship between brain asymmetry and Alzheimer's disease and other dementias previously observed¹⁸⁻²¹. As a separate recurring theme, we found that demographic factors, such as age and sex, are more strongly linked to the amount of brain asymmetry change, not directional change. By contrast, tangible behaviour and lifestyle markers, such as retirement and social interaction proxies, were more closely linked to directional rather than magnitude of asymmetry changes.

Different asymmetry patterns do not all tell the same story. Rather, particular brain patterns of distributed local changes shed unique angles of light onto brain-behavioural correspondence in the context of longitudinal progression of brain structure. For example, directional change in asymmetry pattern 2 was specifically tied to hospitalisation for infectious disease in the intestine. Directional change in pattern 19 was specifically tied to the act of retiring. More research is needed to disentangle how distinct aspects of major life transitions, which have repercussions on social, environmental, psychological, physical aspects of life, relate to brain asymmetry changes, with perhaps special emphasis on the various brain regions that are implicated in asymmetry pattern 19, such as tapetum, temporal occipital fusiform gyrus, and anterior parahippocampal gyrus. Separate lines of inquiry into other major life events, including but not limited to parenthood, finishing university studies, moving to a new city, children leaving home ("empty nest syndrome"), and concurrent brain asymmetry changes may serve as a fruitful extension to retirement-related findings presented herein. Such future research may provide even more insights into how experiencing a period of rapid (external) change may be reflected in observed (internal) brain asymmetry changes.

On a technical data science note, flipping the signs of LBACs neither changes the magnitude of asymmetry change (MBAC) nor the contribution of individual brain features that compose the asymmetry pattern. Furthermore, it should be noted that none of the 33 examined asymmetry patterns represents exclusively either relatively higher or lower volume in a single hemisphere²⁸. Therefore, though an LBAC may be associated with faster volume decline in left cortical grey matter relative to the right cortical grey matter overall, this does not mean that left greater than right imbalance applies for all regional asymmetries that contributes to the overall brain asymmetry pattern. The

stated direction of change also should not be read as a comment on the final structural imbalance between hemispheres. For example, a brain feature which displays L > R asymmetry at baseline and undergoes asymmetry correlated with greater left hemisphere decline may still exhibit L > R asymmetry at the follow-up imaging visit, albeit to a smaller extent. In addition, no asymmetry pattern covers exclusively grey matter but rather, our asymmetry patterns tend to concurrently consider hemispheric asymmetries spanning cortical and subcortical grey matter, major white matter tracts, and cerebellar grey and white matter. Therefore, this reference measure is meant only to aid interpretability, but cannot comment on the hemispheric bias of any individual grey matter homologue, or on the hemispheric biases of single cerebellar regions or white matter tracts.

In parallel to our longitudinal work, many recent large-scale investigations of structural asymmetry have investigated crosssectional variation in brain asymmetry. Perhaps the most welldocumented structural brain asymmetry is the brain torque: it broadly refers to the tendency of human brain anatomy to have concurrent left-occipital and right-frontal volume enlargements and positional shifts (petalia) compared to the contralateral hemisphere⁵⁹. In a large-scale study examining brain torque, Zhao and colleagues found a tendency for older individuals to display more pronounced torque-related asymmetries than younger individuals51. These investigators also outline a similar tendency for more pronounced torqueasymmetry in males versus females⁵¹. In our asymmetry pattern 1, which is the brain asymmetry pattern which bears closest resemblance to the brain torque²⁸, our longitudinal findings suggested an overall trend towards more pronounced brain torque in individuals over time. This trend was stronger in females as compared to males, and in individuals who were older as compared to younger at baseline. Other researchers conducting a meta-analysis examining over 17,000 individuals pooled across 99 datasets revealed non-overlapping sex effects in surface area but not thickness asymmetries⁴⁸. Their investigations failed to find cross-sectional age effects on asymmetry in datasets with an age range of > 5 years. It was only in examining datasets with an age range of 20 years that age effects were observed⁴⁸. By contrast, in our work, we were able to identify longitudinal changes in brain asymmetry which occur over the course of 2 years. These longitudinal changes were linked not only to sex and age (for example, the finding of greater absolute asymmetry change (MBAC) in older individuals relative to younger individuals), but also to non-age-related variables, such as employment status, cognitive performance (and change therein), and mental health.

The divergence between our discovered longitudinal asymmetryphenotypic links and previous cross-sectional studies, both in degree and in kind, are likely reflective of a broader difference in the methodological underpinnings behind these works. Cross-sectional analyses are undoubtedly an invaluable tool in brain research, and provide relatively quick and cost-effective evaluations of brain aging, asymmetry, and other brain phenotypes of interest. Compared to longitudinal results such previous findings tend to underestimate agerelated trends, and are struggling to distinguish between age-related and non-age-related determinants of brain change 7,60,61. In dedicated models predicting individual-level changes in MRI-derived brain measures, models leveraging cross-sectionally-derived trajectories have been found to perform only marginally better than naïve models predicting no change⁷. In fact, non-age-related factors may outweigh the impact of age in tracking longitudinally-acquired empirical rates of brain change in individuals^{7,61}.

Our present longitudinal study has shown that multiple components of brain asymmetry interact in complex ways, and highlights the challenges in understanding brain asymmetries using cross-sectional data alone. Through a naturalistic experiment enabled by the relative older age of our cohort, we revealed that retirement, a major life transition event, was associated with

altered asymmetry changes in specific brain patterns. Furthermore, we showed that this association, as well as associations with phenotypic variables including indicators of mental health. cognitive ability, and socioeconomic status, may exceed associations of brain asymmetry to phenotypes typically linked to brain asymmetry, such as age and sex. Future research aimed at younger cohorts could benefit from similar naturalistic settings, examining how meaningful life events-such as moving out, graduation, or starting a new career-affect brain asymmetry progression. Such studies may for example reveal whether these other life events co-occur with specific changes in brain asymmetry pattern 19, integrating asymmetries in temporal occipital fusiform gyrus, middle frontal gyrus, anterior parahippocampal gyrus, tapetum, and posterior thalamic radiation fibre tracts, which we linked to recent retirement but not stable employment scenarios. Furthermore, this effort could benefit from parallel functional studies in humans that explore the short- and longterm repercussions of incisive life events.

The known differences between results from cross-sectional and longitudinal analyses have repercussions beyond the realm of brain asymmetry, and suggest that existing and on-going cross-sectional investigations aimed at understanding brain change over time (for example, brain-age studies or normative modelling) would benefit from parallel longitudinal investigations in order to benchmark predicted trajectories obtained from between-individual measurements (cross-sectional) against those obtained from within-individual (longitudinal) measurements.

A limitation of this and other longitudinal MRI-based studies is the potential confounds of behaviours outside those under investigation. For example, short-term activity (finger tapping) can result in differences in grey matter volume estimates⁶². In-scanner visual conditions can result in apparent morphological changes in areas linked to the visual cortex⁶³. Finally, diurnal fluctuations may be reflected in different brain activity throughout the day⁶⁴. Though traditionally investigated in the context of brain function⁶⁵, there is emerging evidence that time of day may also influence apparent grey matter volume estimates⁶⁶. Therefore, longitudinal studies would benefit from taking steps to ensure that individual patients are scanned at roughly the same time of day across visits, and that in cross-sectional studies, all individuals be scanned at the same time of day⁶⁶. Overall, integrative research combining cross-sectional with longitudinal studies will not only validate existing knowledge but also pave the way for more precise and functional insights into brain asymmetry and its role in behaviour, health and disease.

Evolutionarily uniquely evolved brain asymmetries appear to be strongly shaped by many non-genetic mechanisms⁶⁷⁻⁶⁹; neither are they static. In-depth explorations into within-subject changes in asymmetries in brain morphology over the span of years, we revealed that structural asymmetry is a dynamic rather than inert property of the brain. Our results further reveal the interdependences of external experiences with internal brain adaptations. We find that changes in hemispheric balance between brain regions are closely tied into health and disease: behaviour, cognitive performance, socioeconomic status, and lifestyle as well as mental and physical medical conditions. These connections in some cases exceed the relationship between structural asymmetry change and ubiquitously studied demographic factors, such as age and sex. In light of these multifaceted dynamics, our population neuroscience study emphasizes the relevance of asymmetry changes in understanding behaviour and highlights the necessity of longitudinal research in comprehending the brain's adaptation to diverse life events.

Methods

Population data source

The UKBB is an epidemiological cohort initiative that offers extensive behavioural and demographic assessments, medical and cognitive measures, as well as biological samples for ~500,000 participants recruited from across Great Britain (https://www.ukbjobank.ac.uk/). This openly accessible population dataset aims to provide multimodal brain-imaging for ~100,000 individuals, originally planned for completion in 2022. Initial MRI brain scanning for participants began being collected in 2014 onwards. Repeat brain-imaging visits commenced in 2019. The present analyses were conducted under UK Biobank application number 25163. Participants were not typically given financial incentives, and informed consent was obtained for all participants. Comprehensive ethical approval has been granted to the UK Biobank project by the North West Multi-Centre Research Ethics Committee application 11/NW/0382, ensuring the study's adherence to high ethical standards (https://www.ukbiobank.ac.uk/learn-more-about-ukbiobank/governance/ethics-advisory-committee). Additional information on the consent procedure is available through the UKBB (https:// biobank.ctsu.ox.ac.uk/crystal/field.cgi?id=200). Our present study was based on the data release from February 2020 that augmented brain scanning information to ~ 40,000 participants (48% male). Participants were aged 40-69 years when recruited (mean age 55, standard deviation [SD] 7.5 years). Of these ~ 40,000 participants, a subset of 1425 (49% male) participants were scanned on two occasions that were 2-3 years apart.

In an attempt to improve comparability and reproducibility, our study built on the uniform data preprocessing pipelines designed and carried out by FMRIB, Oxford University, UK70. Participants in the UKBB underwent homogeneous data collection and processing pipelines as described before⁷¹. Resultant brain imaging measures were made available to researchers in the form of expert-curated imagederived phenotypes (IDPs). Such IDPs span several complementary brain-imaging modalities. As our study aimed to specifically investigate structural asymmetries, we drew on carefully curated IDPs related to grey matter morphology captured by T1-weighted structural magnetic resonance imaging (sMRI) and white matter morphology captured by diffusion-weighted magnetic resonance imaging (dMRI). dMRI-derived measures, made available by the UKBB Imaging team. quantify microstructural aspects of major white matter connections (see Miller et al. 71 for a review of dMRI modalities). Relying on common practices, we elected to use only one kind of dMRI-derived IDPs: fractional anisotropy (FA), which is typically described as a sensitive measure of white matter integrity71. The final collection totalled to 184 anatomical target structures, combined three different reference atlases with brain-derived information: (i) 111 cortical/subcortical volumes (Harvard-Oxford atlas), (ii) 48 major white matter tract integrities (John-Hopkins University atlas), and (iii) 25 cerebellum lobe volumes (Diedrichsen atlas).

Data integrity and quality control was undertaken by the UKBB team. In our present study, participants who underwent two imaging scans were selected. Of these, any participant with no IDPs for a given modality of interest for either visit was discarded from downstream analysis. For example, any participant with sMRI IDPs related to region volume but no dMRI IDPs related to white matter FA was excluded from further analysis. In total, our dataset consisted of 1425 participants (695 male) with biologically interpretable measures drawn from three commonly used anatomical reference atlases.

Construction of whole-brain asymmetry patterns

Quantification of individual-level structural brain asymmetry capitalised on previously established whole-brain asymmetry patterns, which directly integrate structural asymmetries across cerebellum, cortex, subcortex and white matter structure into holistic measures of whole-brain structural asymmetries. Full details on the creation and characterisation of top patterns are available in the work by Saltoun and colleagues (2023) and are summarised below.

In brief, structural brain information from homologous brain pairs (170 brain areas; hence 85 homologous pairs) are unified into 85

unitless lateralisation indices capturing the relative left-right imbalance. These lateralisation indices span cortical (48 pairs) and subcortical (7 pairs) volumes (Harvard-Oxford atlas), white matter tracts (21 pairs) ((John-Hopkins University atlas), and cerebellar volumes (9 pairs) (Diedrichsen atlas). Mathematically, the lateralisation index (LI) of each pair of corresponding homologous atlas parcels was computed as the normalised difference between the right (R) and left (L) homologues according to Eq. 1.

$$LI = \frac{R - L}{\frac{1}{2}(R + L)} \tag{1}$$

Once computed, the lateralisation indices were normalised and corrected for technical deconfounds in accordance with previous work on the UKBB^{54,72}. These technical confound variables comprised head and body size, head motion at task, head motion at rest, head position in the scanner, and scan site. In the present study, normalisation and technical coefficients were identical to those used in Saltoun and colleagues (2023), and were obtained from confound modelling on the baseline MRI scans of a participant set of 37.441 individuals (17.537 male). After this stage of technical deconfounding, the nuisanceadjusted LI metrics were further normalised using Z-scoring, with Z-score parameters obtained from baseline MRI scans of a participant set of 37,441 individuals (17,537 male), to ensure maximal comparability with previous work by Saltoun and colleagues (2023). Once obtained, the nuisance-adjusted, z-score-transformed LI metrics were transformed into individual-level whole-brain asymmetry pattern expressions, according to the publicly available, pre-defined asymmetry pattern definitions²⁸.

Asymmetry patterns were originally obtained from singular value decomposition of the laterization indices for 37,441 individuals (17,537 male) acquired at baseline²⁸. Conceptually, these asymmetry patterns represent sets of brain features whose consistently show joint asymmetry changes. That is, when brain feature A is asymmetric, that is linked with a concurrent change in the asymmetry of brain feature B. Mathematically, asymmetry patterns $P \in \mathbb{R}^{n \times 33}$ are defined in Eq. 2

$$P = A \cdot V$$
 (2)

where $A \in \mathbb{R}^{n \times 85}$ is the LI metrics for all n = 1425 individuals, and $V \in$ R^{85x33} is the pre-defined, publicly available asymmetry pattern definitions. These pattern definitions V indicate the degree and direction of correlated asymmetry the 85 brain features. In the above example, if every leftward bias in brain feature A was correlated with twice the amount of rightward bias in brain feature B across the population, the asymmetry pattern would be $V_{[A,B]} = [-0.05, 0.1]$. The asymmetry pattern expression for a particular individual captures how strongly this specific pattern is manifested in that person's brain. For example, two people with asymmetries $A_{1[A,B]} = [-0.075, 0.15]$ and $A_{2[A,B]} = [0.025, -0.05]$ would have asymmetry pattern expressions of 1.5 and -0.5; which indicates the amount and direction of this particular asymmetry pattern in each individual. Asymmetry patterns capture consistent and concise structural covariation within the asymmetry of brain features across the brain by respecting and incorporating the natural covariation of asymmetries across the brain.

A robustness test conducted by Saltoun and colleagues identified 33 asymmetry patterns which explained more variation in structural asymmetry than would be expected by chance²⁸. In the present work, we built on the definition of these 33 robust asymmetry patterns to conduct our evaluation of asymmetry pattern change across the population. To this end, the asymmetry pattern definitions V for these 33 patterns was extracted and used as templates to quantify the expression with an individual's specific brain asymmetry profile at two time points to then calculate asymmetry pattern change over time (cf. next section).

Two complementary notions of asymmetry change

Individual-level pattern expression P was obtained through Eq. (2) on the basis of publicly available pattern definitions V and individual-level LI expression of 85 brain features (cf. above). The procedure for obtaining asymmetry pattern expression P was carried out as described above identically for both time points, yielding a total of 33 asymmetry pattern expression measurements for 1425 individuals at 2 timepoints per individual.

Within all individuals, the expression levels of a particular asymmetry pattern was compared across timepoints. That is, the expression strength of a given asymmetry pattern at baseline P_1 , was compared to the expression strength of the same asymmetry pattern in the same person at the follow – up visit P_2 . To account for variation in the time intervening between subsequent scans, changes in the asymmetry pattern were further adjusted for the number of days between visits to acquire a yearly rate of asymmetry pattern change. Overall, the longitudinal change in expression of an asymmetry pattern k in a person is given by the following:

$$\Delta P_k = \frac{P_{k_2} - P_{k_1}}{t_{[days]}} * 365 \frac{days}{year}$$
 (3)

More precisely, the quantity ΔP_k represents the lateralized brain asymmetry change (LBAC) of asymmetry pattern k, which captures the directional shift in brain asymmetry. That is, the LBAC quantifies instances where hemispheric homologues display larger lefthemispheric bias with time separately from instances where a larger right-hemispheric bias with time. As a complementary viewpoint on what matters in brain asymmetry, the degree of asymmetry was also captured in a measure that we referred to as the magnitude of brain asymmetry change (MBAC). The MBAC quantifies instances where the brain becomes more structurally asymmetric (positive MBAC) separately from those where the brain becomes less structurally asymmetric (negative MBAC). This is done without regard for whether, as an example, the increase of structural asymmetry was the result of existing left-biased structural asymmetries becoming more pronounced (increasing left-bias LBAC), or from a homologous pair that is symmetric at baseline later displaying an asymmetry corresponding to a larger right-hemisphere homologue (increasing rightbias LBAC). In the previous examples, two opposing directions of asymmetry change (LBAC) resulted in the same macroscopic trend of increased magnitude of brain asymmetry (MBAC).

Mathematically, these target quantities of scientific interest are related to the quantity ΔP_k described above as follows:

LBAC_k =
$$\Delta P_k = \frac{P_{k_2} - P_{k_1}}{\Delta t_{[days]}} * 365 \frac{days}{year}$$
 (4)

and

MBAC_k =
$$|\Delta P_k| = \frac{|P_{k_2} - P_{k_1}|}{\Delta t_{[days]}} * 365 \frac{days}{year}$$
 (5)

The two measures of brain asymmetry offer complementary viewpoints into the morphological asymmetry changes of particular brain features. The MBAC measure considers whether the total amount of asymmetry in the brain has increased or decreased, whereas the LBAC measure considers which hemisphere experienced larger relative shifts in brain volume (grey matter) or structural integrity (white matter). Across the population, these measures diverge from each other if, for example, asymmetry patterns may consistently become more pronounced over time (positive MBAC values indicating larger degrees of absolute asymmetry over time) but individually this asymmetry manifesting as a combination of some individuals whose

asymmetry becomes more right-hemisphere biased while in others the brain becomes more left-hemisphere biased. Hence, the two perspectives on brain asymmetry thus allowed us to disentangle how the brain changes (LBAC) from how much the brain changes (MBAC).

As a final point, the interpretability of LBAC measures was assisted by means of a reference measure. Broadly, LBACs were set up such that positive-valued LBACs correspond to larger cortical grey matter decrease in the left hemisphere as compared to the right hemisphere. To this end, the cortical grey matter in each hemisphere was assessed by taking the sum of all 48 Harvard-Oxford atlas-identified cortical grey volumes for each hemisphere (96 total volumes) for each time point. The total hemispheric cortical grey matter volume (G_R and G_L for the right and left hemisphere, respectively) was compared at each time point. The change in grey matter volume for each hemisphere was calculated as

$$\Delta G_H = G_{H_2} - G_{H_3} \tag{6}$$

where G_H is the cortical grey matter volume for a given hemisphere H, and G_{H_2} is the cortical grey matter volume at timepoint 2 for hemisphere H. Once the change in cortical grey matter volume was obtained for both hemispheres, the relative rate of cortical grey matter volume change was assessed as following

$$\Delta G_{\Delta} = \frac{\Delta G_R - \Delta G_L}{\Delta t_{[aays]}} * 365 \frac{days}{year}$$
 (7)

where ΔG_{Δ} is a measure of the asymmetry of cortical grey matter volume change between hemispheres. If both hemispheres show enlargement of cortical grey matter volume over time ($\Delta G_R > 0$ and $\Delta G_1 > 0$) then the quantity ΔG_{Λ} would be positive if the right hemisphere experiences greater grey matter volume gains than the left hemisphere over the same period of time. If the cortical grey matter volume shrinks in both hemispheres over time ($\Delta G_R < 0$ and $\Delta G_I < 0$), then the quantity ΔG_{Δ} would be positive if the volume decline observed in the left cortex is faster than the volume decline observed in the right cortex (mathematically, if ΔG_L is more negative than ΔG_R). This whole-cortex measure of relative hemispheric volume change serves as the yardstick we used to contextualise LBAC measures. The sign of the LBAC measures was adjusted such that LBAC measures are positively correlated with a positive ΔG_{Δ} quantity. That is, positive LBAC measures indicated faster cortical volume growth in the right hemisphere, or equivalently, faster cortical volume decline in the left hemisphere.

A curated phenome of target behavioural phenotypes

In order to ground our computed indices of LBACs and MBACs in potential real-world implications, we performed a rich annotation of the derived asymmetry pattern changes, benefitting from a wide variety of almost 1400 lifestyle factors, behavioural changes, demographic indicators, and mental health assessments. These ~1400 are subdivided into ~1000 baseline behavioural phenotypes as well as ~400 behavioural changes which contrast behaviour and lifestyle at imaging visits 1 and 2.

Baseline behavioural phenotypes were extracted in the identical manner as described in previous work by Saltoun and colleagues (2023). As a broad overview, feature extraction for 'baseline' behaviour was carried out using two utilities designed to obtain, clean and normalise UKBB phenotype data according to predefined rules. Initially, a raw collection of ~15,000 phenotypes was fed into the FMRIB UKBB Normalisation, Parsing And Cleaning Kit (FUNPACK version 2.5.0; https://zenodo.org/record/4762700#.YQrpui2caJ8). FUNPACK was used to carefully curate a collection of phenotypes associated with the categories of interest and conduct data harmonisation. The output of FUNPACK, consisting of ~3300 phenotypes, was then input into

PHEnome Scan Analysis Tool (PHESANT;⁷³, https://github.com/MRCIEU/PHESANT) for further refinement, cleaning and data categorisation. The final set of 977 baseline phenotypes obtained from PHESANT was tested for systematic relations to the discovered asymmetry pattern changes (i.e., LBAC, MBAC) to explore possible relations between brain asymmetry change and behaviour.

More specifically, we used FUNPACK on the UKBB sample to extract phenotype information covering 11 major categories, ranging from lifestyle to mental health and cognitive phenotypes to blood pressure measurements. These categories of interest were predefined in the FUNPACK utility through the -cfg fmrib arguments. They included only lifestyle phenotypes and excluded any brain-imaging-derived information. As there were only four phenotypes associated with diet, we discarded this category from downstream analysis. The FUNPACK setting, which defined categories, also contained built-in rules tailored to the UKBB. This tool performed automated refinements of the phenotype data, such as ruling out 'do not know' responses and replacing unasked dependent data. For example, a participant who indicated that they do not use mobile phones was not asked how long per week they spent using a mobile phone. In this case, FUNPACK would fill in a value of zero hours per week as a response to the latter question, though a value was not obtained at the time of assessment. FUNPACK's thus built-in rules pipeline yielded 3330 curated phenotype columns.

The FUNPACK output was then feed into PHESANT, a tool designed specifically for curating UKBB phenotypes⁷³, https://github.com/MRCIEU/PHESANT). The PHESANT toolkit combined phenotypes across visits, normalised, cleaned and categorised the data as belonging to one of four datatypes: categorical ordered, categorical unordered, binary and numerical. All categorical unordered columns were converted into binary columns to encode a single response. For example, the employment status phenotype was originally encoded as a set of values representing different conditions (e.g., retired, employed, on disability). Each of these conditions was converted into a binary column (e.g., retired true or false). The output of categorical one-hot encoding on unordered phenotypes was then combined with all measures classified by PHESANT as binary, numerical, or categorical ordered. The final set comprised carefully curated 977 phenotypes.

We deployed both FUNPACK and PHESANT with their default parameter choices regarding missing data on the full set of ~40,000 individuals with brain-imaging scans at the initial imaging visit. As a consequence, all columns with fewer than 500 participants were automatically discarded from further analysis as per PHESANT's workflow protocols. In addition, FUNPACK by default assessed pairwise correlation between phenotypes and discarded all but one phenotype of a set of highly correlated (> 0.99 Pearson's correlation rho) phenotypes. For example, left and right leg fat percentages were highly correlated (Pearson's rho 0.992). Hence, only the right leg fat percentage was included in the final set of phenotypes. The choices which phenotypes to discard were also automatically streamlined and conducted by FUNPACK.

Change of target behavioural phenotypes

To complement our measures of longitudinal change in brain morphology (cf. above), we aimed to also create measures of intra-subject change in our behavioural phenotypes (henceforth, behaviour change). Feature extraction for behavioural 'change' phenotypes underwent a similar procedure as for 'baseline' behavioural indicators. Measures of behavioural change were obtained for behaviours and phenotypes which measured at both imaging visits in the same subject. As before, both FUNPACK and PHESANT were utilised in conjunction, with the same set of categories extracted as for 'baseline' behaviour. However, slight adjustments were necessary into order to enable the comparison of behavioural response variables across time. Therefore, a number of steps, detailed below, were taken to ensure that

behavioural responses from imaging visit 1 are comparable to behavioural responses from imaging visit 2 in the UK Biobank imaging cohort.

Part of PHESANT's standard pipeline is the integration of behavioural responses across timepoints. As our goal was to contrast a snapshot of behaviour at imaging visit 1 with a snapshot of behaviour at imaging visit 2, we separately fed imaging visit 1 behaviour and visit 2 behaviour into PHESANT. FUNPACK was used to extract phenotypes collected at each respective visit prior to being fed into PHESANT. A separate feature of PHESANT's standard pipeline is the automatic normalisation applied to categorical variables. As our goal was to compare phenotypes at visits 1 and 2, normalisation procedures applied separately to each visit may obfuscate behavioural change. Hence, PHESANT's normalisation procedure was suppressed using the 'standardise = FALSE' argument, with manual cheques to verify that input values matched output variables after PHESANT was run. A third consideration in ensuring comparability between behavioural phenotypes at each visit related to PHESANT's automatic categorisation of phenotypes into categorical (ordered), categorical (unordered), binary, or continuous. For some phenotypes, the behaviour at one time point was categorised as categorical (ordered or unordered) but binary in another time point. In instances where different encoding was used on the same behaviour from different timepoints, behaviour from timepoint 2 was manually recoded according to the rules PHE-SANT automatically applied to behaviour at timepoint 1.

Once behaviour at each timepoint was acquired, a measure of behavioural change was acquired through the following:

$$\Delta \Phi = \Phi_2 - \Phi_1 \tag{8}$$

where $\Delta\Phi$ is the behaviour change of phenotype Φ , and Φ_2 and Φ_1 are the behaviours as recorded at imaging visit 2 and 1 respectively. In the case of binary or categorical phenotypes, a value of '0' indicates no change in behaviour between the two imaging visits. A value of '1' indicates a behaviour which was present at timepoint 2 but not at timepoint 1 (for example, a non-smoker at timepoint 1 who smokes at timepoint 2). A value of '-1' indicates a behaviour which was present at timepoint 1 but absent at timepoint 2. Normalisation to mean 0 and standard deviation 1 was conducted on behavioural change phenotypes for all PHESANT-tagged continuous behaviours. As the total number of participants in the present study was 1425 individuals, PHESANT's native workflow step to remove all behaviours with fewer than 500 participants was suppressed. Behaviours with fewer than 10% response rate at either time point were dropped. In so doing, a total of 396 behavioural change phenotypes spanning 9 domains were extracted through this procedure.

Exploration of asymmetry change linked to life and disease

To get a snapshot of how various aspects of life and behaviour track whole-brain asymmetry changes, we related a given domain of lifestyle or lifestyle change to a measure of brain asymmetry change. To this end, we regressed a given brain asymmetry change (LBAC or MBAC) onto phenotypes from a particular lifestyle domain. To disentangle the impact of common demographic factors from behavioural phenotypes, 6 demographic features (age, sex, age², age*sex, age²*sex, time between visits measured in days) were included in all regressions.

$$LBAC = \beta_0 + \sum_{F \in Demographics} \beta_F * F + \sum_{D \in Domain} \beta_{\Delta \Phi_D} * \Delta \Phi_D$$
 (9)

and

$$MBAC = \beta_0 + \sum_{F \in Demographics} \beta_F * F + \sum_{D \in Domain} \beta_{\Delta \Phi_D} * \Delta \Phi_D$$
 (10)

where F is the full collection of 6 demographic features (age, sex, age², age*sex, age²*sex, time between visits) and D is the set of phenotypes belonging to either a single baseline lifestyle domain, or a single lifestyle change domain. There are a total of 20 groups of analysis (11 baseline domains and 9 change domains).

For all regressions, the coefficient of determination, R^2 , was used as an established performance metric to quantify the amount of variance in brain asymmetry change (model outcome variable) that can be explained by the lifestyle domain at hand (model input variables). As the number of behaviours within a domain depends on the domain at hand, we adjusted the resultant coefficient of determination to account for the number of features in the regressions as follows.

$$R^2 = 1 - \left(1 - R_0^2\right) \frac{n - 1}{n - d - 1} \tag{11}$$

where R_0^2 is the unadjusted coefficient of determination, n is the number of participants, and d is the number of regression features. This formulation is called the adjusted R2 statistic and is widely used when comparing models of different size $\binom{74}{2}$, p. Section 6.1.3).

The results from estimating these linear regression model specifications provide a broad snapshot of how broad lifestyle domains relate to brain asymmetry changes. They were conducted of the 33 measures (i.e., number of previously reported brain asymmetry patterns) of directional brain asymmetry change (LBAC) and amount of brain asymmetry change (MBAC). A final set of regressions without any lifestyle domain (in other words, with only 6 demographic features and intercept as regressors) was carried out, as a null model without behaviour effects to compare against.

We next sought to establish a complementary viewpoint into the relationship between brain asymmetry change and tangible behaviour changes. To this end, we conducted a series of regression analyses which a given behavioural change to underlying brain asymmetry changes and demographic factors.

$$\Delta \Phi = \beta_0 + \sum_{F \in Demographics} \beta_F * F + \sum_{i=1}^{33} \beta_{LBAC_i} * LBAC_i + \sum_{i=1}^{33} \beta_{MBAC_i} * MBAC_i \quad (12)$$

As above, we included a set of 6 demographic factors, which include the time between visits, as covariates within the model. For maximum comparability between linear regressions obtained from this set of analysis to the above set, we reported the adjusted R2 statistic as calculated above.

Behavioural changes have not been corrected for time between visits, and may be strongly related to either age or sex. Therefore, we expect that the included demographic features (age, sex, time between visits) may have an outsized impact on the linear regression. To account for this, we aimed to determine the expected adjusted R2 statistic if there was no impact of brain asymmetry change on the behavioural change at hand. To do this, we have repeated the regression analyses after permuting LBAC and MBAC labels, which breaks the relationship between brain asymmetry change and the behavioural change at hand. The adjusted R2 statistic, which resulted from these regressions, was subtracted out from the adjusted R2 statistic from the unperturbed data. In so doing, we were able to quantify the added benefit of brain asymmetry changes (both LBACs and MBACs) on charting the relationship between behavioural change and brain and demographics.

For visualisation purposes, the largest absolute beta coefficient from the above equation was extracted for each of the 396 separate behavioural change variables, each of which has one regression analysis linking brain change to behaviour change. The feature corresponding to this beta coefficient represents the strongest relationship between the behavioural change of interest and all examined input features. To ensure comparability of beta coefficients, all input features were normalised to mean 0 and standard deviation 1 prior to

conducting the regression. The strongest feature was grouped according to membership of LBAC features, MBAC features, or demographic/intercept term features.

Electronic healthcare record data

To offer a distinct window into a separate field of biological phenotypes which may be linked to morphological between brain asymmetry pattern changes, we turned our attention to physician-diagnosed medical illnesses as captured through electronic health records. To this end, we performed a rich annotation of the derived brain asymmetry pattern changes by means of a phenome-wide association analysis, benefitting from a wide variety of almost 1700 disease phecodes extracted from participants' electronic health records, spanning over 11,000 ICD codes. Feature extraction for both ICD-9 and ICD-10 diagnoses was carried out using the FMRIB UKBB Normalisation, Parsing and Cleaning Kit (FUNPACK version 2.5.0; https://zenodo.org/ record/4762700#.YQrpui2caJ8). Once extracted, ICD-9 and ICD-10 codes were grouped into ~1700 hierarchical phenotypes (phecodes) which combine related ICD-9 and ICD-10 codes into a single 'phecode', using previously established phecode definitions which spanning 17 disease classes⁷⁵. For technical reasons, the full set of ~1700 disease phecodes were condensed using several data compression protocols on a per disease class basis, to create a total of 174 composite disease clusters. These composite disease clusters were finally compared to measures of brain asymmetry pattern change to probe for relations between morphological brain asymmetry changes and clinical diagnoses.

More concretely, we used FUNPACK on the full UKBB cohort (n = 502,507) to extract phenotype information related to ICD-9 diagnosis codes and ICD-10 diagnosis codes. This collection of 502,507 participants contained within it the full imaging cohort $(n \sim 40,000)$ and the repeat imaging cohort (n = 1425). The FUNPACK utility contained built-in rules tailored to the UKBB, which enabled the extraction of a total of 2837 columns associated with ICD-9 codes (2506 unique codes) and 14.217 columns associated with ICD-10 codes (8845 unique codes). These ICD codes were collected on the basis of electronic health records linked to each participant. ICD-10 codes contain more granular information than ICD-9 codes⁷⁵; separate ICD-9 and -10 codes may reflect common etiologies^{76,77}. To consolidate related medical diagnoses across and within ICD coding paradigms, we used the Phecode Map 1.2 with ICD-10 codes made available from Wu and colleagues (https://phewascatalog.org/phecodes_icd10⁷⁵). In total, applying phecode definitions linking ICD codes resulted in a final set of 1662 clinical phecodes obtained from 502,507 participants. These clinical phecodes spanned 17 disparate disease classes, ranging from congenital anomalies, to neoplasms, to mental disorders, to infectious diseases⁷⁵.

For technical reasons, the collection of 1662 clinical phecodes required a further refinement prior to analysis with our set of wholebrain asymmetry changes. To this end, 3 separate data compression techniques were used to reduce the total set of 1662 clinical phecodes into a set of 174 composite disease clusters, which capture distinct underlying trends in the overall diagnosis landscape. For increased interpretability, these composite disease clusters each integrate disease status from phecodes within one disease class only.

As the first data reduction technique, we turned to principal component analysis (PCA), which is a commonly used unsupervised data reduction technique. PCA is an unsupervised method whose extracted latent factors represent the dimensions of maximum variance within the dataset.

We applied PCA on the full UKBB cohort (n > 500,000), rather than the repeat imaging cohort (n = 1425), to improve the representativeness and stability of the resultant composite disease clusters. To boost the interpretability of resultant latent factors, PCA was applied separately to each of the 17 disease classes. In other words,

Table 1 | Disease class size before and after PCA-based data compression

| Disease Category | Number of Phecodes | Number of latent factors | Total Explained Variance of latent factors (%) |
|----------------------------|-----------------------|-----------------------------|--|
| Circulatory System | 155 | 4 | 50.1 |
| Congenital Anomalies | 54 | 1 | 38.3 |
| Dermatological | 94 | 4 | 45.3 |
| Digestive | 155 | 6 | 48.3 |
| Endocrine/Metabolic | 146 | 2 | 51.5 |
| Genitourinary | 156 | 10 | 52.1 |
| Hematopoietic | 54 | 3 | 64.4 |
| Infectious Diseases | 55 | 2 | 44.7 |
| Injuries and Poisonings | 125 | 2 | 21.6 |
| Mental Disorders | 70 | 4 | 64.5 |
| Musculoskeletal | 120 | 2 | 36.0 |
| Neoplasms | 132 | 3 | 39.9 |
| Neurological | 78 | 5 | 53.5 |
| Pregnancy Complications | 44 | 1 | 22.9 |
| Respiratory | 75 | 6 | 64.0 |
| Sense Organs | 113 | 1 | 23.0 |
| Symptoms | 36 | 2 | 46.0 |
| Total | 1662 | 58 | 45.1 (Mean) |

Composite disease clusters (latent factors) are retained for latent factors whose explained variance exceed the explained variance of equivalent noise-based latent factors. PCA was applied separately for each disease class.

PCA was applied 17 times, with each PCA application being specific to phecodes within a single disease class. The interpretability of latent factors thus boosted because each latent factor is intrinsically linked to only one aspect of health. For example, the latent factor obtained from applying PCA to phecodes in the mental health disorders disease class represents clinical diagnoses within the mental health domain only, irrespective of diagnoses in other domains. This enables an at-a-glance insight into the content of the latent factor based on which disease category it captures. By contrast, PCA applied on the full set of 1,662 clinical phecodes at once would combine phecodes from across disease classes, which may make it more difficult to separate the effects of diseases in one class, such as mental health disorders, from diseases in another class, such as endocrine/metabolic disorders.

For each of the 17 disease clusters, the question of how many latent factors to keep was addressed by means of label-wise permutation testing. To break the link between related disease phecodes, we perturbed each of the clinical phecodes within a disease cluster separately, before applying PCA on the permuted dataset. This enabled us to establish the expected explained variance in a scenario where there is no relationship between separate disease phecodes. A total of 5 permutations was done for each disease category, and the mean explained variance for each noise-based latent factor was taken as a reference measure. Unperturbed (true) latent factors were kept if their explained variance exceeded the explained variance of the equivalent noise-based latent factor. This procedure resulted in a total of 58 latent factors spanning 17 disease classes being retained, with the per-class latent factors ranging from one, in the case of the pregnancy complications and congenital anomality disease classes, to ten, in the case of genitourinary diseases (Table 1). On average, the retained latent factors explained 45.1% of the variance within their respective disease class (Table 1).

To complement the PCA-derived composite disease clusters, we used two doubly multivariate latent factor decomposition methods to establish latent factors which explicitly link disease status to brain activity. Specifically, we used canonical correlation analysis (CCA) and canonical partial least squares (PLS-C) decomposition. Both these self-supervised methods are doubly multivariate, meaning that they integrate information from one 'block' of variables, in this case disease status, with another 'block' of variables. We capitalise on the resting-state fMRI data available through the UKBB to establish composite disease clusters which link resting-state brain activity (one 'block') to clinical phecodes (the second 'block'). Resting-state functional imaging was acquired over the course of 6 minutes for 37,526 participants. For technical reasons to avoid overfitting, we reduced the expertcurated full and partial correlation matrices (dimensions 25 and 100) made available by the UKBB team to 100 top PC components prior to applying dimensionality reduction techniques, in accordance with standard practice [Nichols positive negative]. As with PCA, both CCA and PLS-C were conducted on each disease class separately. The number of latent factors kept for each technique was equivalent to the number of latent components identified in the PCA analysis. That is, if the PCA analysis resulted in 3 latent factors for a given disease class, the top 3 CCA and top 3 PLS-C latent factors for that disease class were kept. In this way, we extracted an additional set of 116 composite disease clusters (58 each for CCA and PLS-C) from our original set of clinical phecodes. These composite disease clusters linked resting state brain activity (as captured in fMRI imaging) to disease status (as captured in clinical phecodes), and thus represented a different dimension of disease.

Finally, we charted robust cross-links between the subjectwise expression of a given brain asymmetry pattern change and the portfolio of 174 composite disease clusters, with appropriate correction for multiple comparisons. For each composite disease clusters, the Pearson correlation between the given composite disease clusters and the inter-individual variation in brain asymmetry change revealed both the association strength and accompanying statistical significance of the given disease clusterbrain asymmetry change association. For each uncovered brain asymmetry pattern change, two standard tests were used to adjust for the multitude of associations being assessed. First, we used Bonferroni's correction for multiple comparisons, adjusting for the number of tested phenotypes (0.05/174 = 2.87e-4). Second, we further evaluated the significance of our correlation strength using the false discovery rate (FDR), another popular method of multiple comparison correction which is less stringent than Bonferroni's correction. The false discovery rate⁷⁸ was set as 5%71,79,80 and computed in accordance with standard practice⁸¹. For visualisation purposes, disease clusters in Manhattan plots were coloured and grouped according to the category membership defined by the phecode map developed by Wu and colleagues (2019) and shape in accordance to the dimension reduction technique applied. This procedure was applied for measures capturing direction of brain asymmetry change (LBACs) as well as magnitude of brain asymmetry change (MBACs).

Reporting summary

Further information on research design is available in the Nature Portfolio Reporting Summary linked to this article.

Data availability

Individual-level data are under controlled access to protect the sensitive information of the study participants, and may be requested by

application to the UKBB (https://www.ukbiobank.ac.uk/enable-your-research/register). Processed data is available upon request. Source data are provided in this paper.

Code availability

The processing scripts and custom analysis software used in this work are available in a publicly accessible GitHub repository along with examples of key visualisations in the paper: https://github.com/ksaltoun/asympath_age_progression/. They are also available through Zenodo at: https://doi.org/10.5281/zenodo.15392168⁸².

References

- Zatorre, R. J., Fields, R. D. & Johansen-Berg, H. Plasticity in gray and white: neuroimaging changes in brain structure during learning. *Nat. Neurosci.* 15, 528–536 (2012).
- May, A. Experience-dependent structural plasticity in the adult human brain. *Trends Cogn. Sci.* 15, 475–482 (2011).
- Boyke, J., Driemeyer, J., Gaser, C., Buchel, C. & May, A. Traininginduced brain structure changes in the elderly. J. Neurosci. 28, 7031–7035 (2008).
- 4. Draganski, B. et al. Neuroplasticity: changes in grey matter induced by training. *Nature* **427**, 311–312 (2004).
- Taubert, M. et al. Dynamic properties of human brain structure: learning-related changes in cortical areas and associated fiber connections. J. Neurosci. 30, 11670–11677 (2010).
- Tavor, I., Botvinik-Nezer, R., Bernstein-Eliav, M., Tsarfaty, G. & Assaf, Y. Short-term plasticity following motor sequence learning revealed by diffusion magnetic resonance imaging. *Hum. Brain Mapp.* 41, 442–452 (2020).
- Di Biase, M. A. et al. Mapping human brain charts cross-sectionally and longitudinally. Proc. Natl. Acad. Sci. USA 120, e2216798120 (2023).
- Deary, I. J., Penke, L. & Johnson, W. The neuroscience of human intelligence differences. Nat. Rev. Neurosci. 11, 201–211 (2010).
- Kanai, R. & Rees, G. The structural basis of inter-individual differences in human behaviour and cognition. *Nat. Rev. Neurosci.* 12, 231–242 (2011).
- Tang, Y. Y. et al. Short-term meditation induces white matter changes in the anterior cingulate. *Proc. Natl. Acad. Sci. USA* 107, 15649–15652 (2010).
- Chiang, M. C. et al. Genetics of brain fiber architecture and intellectual performance. J. Neurosci. 29, 2212–2224 (2009).
- Hofstetter, S., Friedmann, N. & Assaf, Y. Rapid language-related plasticity: microstructural changes in the cortex after a short session of new word learning. *Brain Struct. Funct.* 222, 1231–1241 (2017).
- Paul, L. K. et al. Agenesis of the corpus callosum: genetic, developmental and functional aspects of connectivity. *Nat. Rev. Neu*rosci. 8, 287–299 (2007).
- Shamay-Tsoory, S. G., Aharon-Peretz, J. & Perry, D. Two systems for empathy: a double dissociation between emotional and cognitive empathy in inferior frontal gyrus versus ventromedial prefrontal lesions. *Brain* 132, 617–627 (2009).
- 15. Valk, S. L. et al. Structural plasticity of the social brain: Differential change after socio-affective and cognitive mental training. *Sci. Adv.* **3**, e1700489 (2017).
- Hartwigsen, G., Bengio, Y. & Bzdok, D. How does hemispheric specialization contribute to human-defining cognition? *Neuron* 109, 2075–2090 (2021).
- Stein, M. et al. Structural plasticity in the language system related to increased second language proficiency. Cortex 48, 458–465 (2012).
- Kumfor, F. et al. On the right side? A longitudinal study of leftversus right-lateralized semantic dementia. *Brain* 139, 986–998 (2016).
- Cherbuin, N., Reglade-Meslin, C., Kumar, R., Sachdev, P. & Anstey, K. J. Mild cognitive disorders are associated with different patterns

- of brain asymmetry than normal aging: The PATH through life study. *Front. Psychiatry* **1**, 11 (2010).
- Haxby, J. V. et al. Longitudinal study of cerebral metabolic asymmetries and associated neuropsychological patterns in early dementia of the Alzheimer type. Arch. Neurol. 47, 753–760 (1990).
- Wachinger, C., Salat, D. H., Weiner, M., Reuter, M. & Alzheimer's Disease Neuroimaging, I. Whole-brain analysis reveals increased neuroanatomical asymmetries in dementia for hippocampus and amygdala. *Brain* 139, 3253–3266 (2016).
- Sarica, A. et al. MRI Asymmetry index of hippocampal subfields increases through the continuum from the mild cognitive impairment to the Alzheimer's disease. Front. Neurosci. 12, 576 (2018).
- Assaf, Y. New dimensions for brain mapping. Science 362, 994–995 (2018).
- Caroni, P., Donato, F. & Muller, D. Structural plasticity upon learning: regulation and functions. *Nat. Rev. Neurosci.* 13, 478–490 (2012).
- Lerch, J. P. et al. Maze training in mice induces MRI-detectable brain shape changes specific to the type of learning. *Neuroimage* 54, 2086–2095 (2011).
- Blumenfeld-Katzir, T., Pasternak, O., Dagan, M. & Assaf, Y. Diffusion MRI of structural brain plasticity induced by a learning and memory task. PLoS ONE 6, e20678 (2011).
- Sagi, Y. et al. Learning in the fast lane: new insights into neuroplasticity. Neuron 73, 1195–1203 (2012).
- 28. Saltoun, K. et al. Dissociable brain structural asymmetry patterns reveal unique phenome-wide profiles. *Nat. Hum. Behav.* **7**, 251–268 (2023).
- Fotenos, A. F., Snyder, A. Z., Girton, L. E., Morris, J. C. & Buckner, R. L. Normative estimates of cross-sectional and longitudinal brain volume decline in aging and AD. *Neurology* 64, 1032–1039 (2005).
- Cole, J. H. & Franke, K. Predicting age using neuroimaging: Innovative brain ageing biomarkers. *Trends Neurosci.* 40, 681–690 (2017).
- Driscoll, I. et al. Longitudinal pattern of regional brain volume change differentiates normal aging from MCI. *Neurology* 72, 1906–1913 (2009).
- Franke, K., Ziegler, G., Kloppel, S., Gaser, C. & Alzheimer's Disease Neuroimaging, I. Estimating the age of healthy subjects from T1weighted MRI scans using kernel methods: exploring the influence of various parameters. *Neuroimage* 50, 883–892 (2010).
- 33. Kiesow, H. et al. 10,000 social brains: Sex differentiation in human brain anatomy. *Sci. Adv.* **6**, eaaz1170 (2020).
- Ritchie, S. J. et al. Sex differences in the adult human brain: Evidence from 5216 UK biobank Participants. Cereb. Cortex 28, 2959–2975 (2018).
- 35. Taki, Y. et al. Correlations among brain gray matter volumes, age, gender, and hemisphere in healthy individuals. *PLoS ONE* **6**, e22734 (2011).
- Blinkouskaya, Y. & Weickenmeier, J. Brain shape changes associated with cerebral atrophy in healthy aging and alzheimer's disease. Front. Mech. Eng. https://doi.org/10.3389/fmech.2021.705653 (2021).
- 37. Hirnstein, M., Hugdahl, K. & Hausmann, M. Cognitive sex differences and hemispheric asymmetry: A critical review of 40 years of research. *Laterality* **24**, 204–252 (2019).
- 38. Nisbett, R. E. et al. Intelligence: new findings and theoretical developments. *Am. Psychol.* **67**, 130–159 (2012).
- Brown, B. C., McKenna, S. P., Siddhi, K., McGrouther, D. A. & Bayat,
 A. The hidden cost of skin scars: quality of life after skin scarring. J. Plast. Reconstr. Aesthet. Surg. 61, 1049–1058 (2008).
- Tripathi, R., Knusel, K. D., Ezaldein, H. H., Scott, J. F. & Bordeaux, J. S. Association of demographic and socioeconomic characteristics with differences in use of outpatient dermatology services in the United States. *JAMA Dermatol.* **154**, 1286–1291 (2018).

- Cryan, J. F. & Dinan, T. G. Mind-altering microorganisms: the impact of the gut microbiota on brain and behaviour. *Nat. Rev. Neurosci.* 13, 701–712 (2012).
- Cryan, J. F. et al. The microbiota-gut-brain axis. Physiol. Rev. 99, 1877–2013 (2019).
- Foster, J. A. & McVey Neufeld, K. A. Gut-brain axis: how the microbiome influences anxiety and depression. *Trends Neurosci.* 36, 305–312 (2013).
- 44. Nicholson, J. K. et al. Host-gut microbiota metabolic interactions. *Science* **336**, 1262–1267 (2012).
- Bercik, P. et al. The intestinal microbiota affect central levels of brain-derived neurotropic factor and behavior in mice. Gastroenterology 141, 599–609 (2011). 609 e591-593.
- Szucs, D. & Ioannidis, J. P. Sample size evolution in neuroimaging research: An evaluation of highly-cited studies (1990-2012) and of latest practices (2017-2018) in high-impact journals. *Neuroimage* 221, 117164 (2020).
- Woo, C. W., Chang, L. J., Lindquist, M. A. & Wager, T. D. Building better biomarkers: brain models in translational neuroimaging. *Nat. Neurosci.* 20, 365–377 (2017).
- 48. Kong, X. Z. et al. Mapping cortical brain asymmetry in 17,141 healthy individuals worldwide via the ENIGMA Consortium. *Proc. Natl. Acad. Sci. USA* 115, E5154–E5163 (2018).
- Kong, X. Z. et al. Large-scale phenomic and genomic analysis of brain asymmetrical skew. Cereb. Cortex 31, 4151–4168 (2021).
- 50. Kong, X. Z. et al. Mapping brain asymmetry in health and disease through the ENIGMA consortium. *Hum. Brain Mapp.* **43**, 167–181 (2022).
- Zhao, L., Matloff, W., Shi, Y., Cabeen, R. P. & Toga, A. W. Mapping complex brain torque components and their genetic architecture and phenomic associations in 24,112 individuals. *Biol. Psychiatry* 91, 753–768 (2022).
- 52. Vingerhoets, G. Phenotypes in hemispheric functional segregation? Perspectives and challenges. *Phys. Life Rev.* **30**, 1–18 (2019).
- 53. Dunbar, R. I. M. The anatomy offriendship. *Trends Cogn. Sci.* 22, 32–51 (2018).
- 54. Schurz, M. et al. Variability in brain structure and function reflects lack of peer support. *Cereb. Cortex* **31**, 4612–4627 (2021).
- Roberts, S. G. & Dunbar, R. I. Communication in social networks: Effects of kinship, network size, and emotional closeness. *Personal. Relatsh.* 18, 439–452 (2011).
- Flicker, L. Modifiable lifestyle risk factors for Alzheimer's disease. J. Alzheimers Dis. 20, 803–811 (2010).
- Fratiglioni, L., Paillard-Borg, S. & Winblad, B. An active and socially integrated lifestyle in late life might protect against dementia. *Lancet Neurol.* 3, 343–353 (2004).
- Shafighi, K. et al. Social isolation is linked to classical risk factors of Alzheimer's disease-related dementias. PLoS ONE 18, e0280471 (2023).
- Toga, A. W. & Thompson, P. M. Mapping brain asymmetry. Nat. Rev. Neurosci. 4, 37–48 (2003).
- Fosse, E. & Winship, C. Bounding analyses of age-period-cohort effects. *Demography* 56, 1975–2004 (2019).
- 61. Lindenberger, U., von Oertzen, T., Ghisletta, P. & Hertzog, C. Crosssectional age variance extraction: what's change got to do with it? Psychol. Aging **26**, 34–47 (2011).
- 62. Olivo, G. et al. Estimated gray matter volume rapidly changes after a short motor task. *Cereb. Cortex* **32**, 4356–4369 (2022).
- Mansson, K. N. T. et al. Viewing pictures triggers rapid morphological enlargement in the human visual cortex. Cereb. Cortex 30, 851–857 (2020).
- Byrne, J. E. M., Hughes, M. E., Rossell, S. L., Johnson, S. L. & Murray, G. Time of days differences in neural reward functioning in healthy young men. *J. Neurosci.* 37, 8895–8900 (2017).

- 65. Orban, C., Kong, R., Li, J., Chee, M. W. L. & Yeo, B. T. T. Time of day is associated with paradoxical reductions in global signal fluctuation and functional connectivity. *PLoS Biol.* **18**, e3000602 (2020).
- Karch, J. D. et al. Identifying predictors of within-person variance in MRI-based brain volume estimates. *Neuroimage* 200, 575–589 (2019).
- 67. Carrion-Castillo, A. et al. Genetic effects on planum temporale asymmetry and their limited relevance to neurodevelopmental disorders, intelligence or educational attainment. *Cortex* **124**, 137–153 (2020).
- 68. Corballis, M. C. The evolution and genetics of cerebral asymmetry. *Philos. Trans. R. Soc. Lond. B Biol. Sci.* **364**, 867–879 (2009).
- Badzakova-Trajkov, G., Haberling, I. S., Roberts, R. P. & Corballis, M. C. Cerebral asymmetries: complementary and independent processes. *PLoS ONE* 5, e9682 (2010).
- Alfaro-Almagro, F. et al. Image processing and Quality Control for the first 10,000 brain imaging datasets from UK Biobank. Neuroimage 166, 400–424 (2018).
- Miller, K. L. et al. Multimodal population brain imaging in the UK Biobank prospective epidemiological study. *Nat. Neurosci.* 19, 1523–1536 (2016).
- 72. Spreng, R. N. et al. The default network of the human brain is associated with perceived social isolation. *Nat. Commun.* **11**, 1–11 (2020).
- Millard, L. A. C., Davies, N. M., Gaunt, T. R., Davey Smith, G. & Tilling, K. Software Application Profile: PHESANT: a tool for performing automated phenome scans in UK Biobank. *Int. J. Epidemiol.* 47, 29–35 (2018).
- 74. James, G., Witten, D., Hastie, T. & Tibshirani, R. *An introduction to statistical learning*. (Springer, 2013).
- 75. Wu, P. et al. Mapping ICD-10 and ICD-10-CM codes to phecodes: Workflow development and initial evaluation. *JMIR Med. Inf.* **7**, e14325 (2019).
- Denny, J. C. et al. Systematic comparison of phenome-wide association study of electronic medical record data and genome-wide association study data. *Nat. Biotechnol.* 31, 1102–1110 (2013).
- Denny, J. C. et al. PheWAS: demonstrating the feasibility of a phenome-wide scan to discover gene-disease associations. *Bioinformatics* 26, 1205–1210 (2010).
- 78. Benjamini, Y. & Hochberg, Y. Controlling the false discovery rate: a practical and powerful approach to multiple testing. *J. R. Stat. Soc. Ser. B* **57**, 289–300 (1995).
- Raizada, R. D., Richards, T. L., Meltzoff, A. & Kuhl, P. K. Socioeconomic status predicts hemispheric specialisation of the left inferior frontal gyrus in young children. *Neuroimage* 40, 1392–1401 (2008).
- 80. Sha, Z. et al. The genetic architecture of structural left-right asymmetry of the human brain. *Nat. Hum. Behav.* **5**, 1226–1239 (2021).
- 81. Genovese, C. R., Lazar, N. A. & Nichols, T. Thresholding of statistical maps in functional neuroimaging using the false discovery rate. *Neuroimage* **15**, 870–878 (2002).
- 82. Saltoun, K., Bzdok, D., Paul, L. K., Yeo, B. T. T. & Diedrichsen, J. Longitudinal structural changes in brain asymmetry track lifestyle and disease. In. Zenodo. https://doi.org/10.5281/zenodo. 15392168 (2025).

Acknowledgements

D.B. was supported by the Brain Canada Foundation, through the Canada Brain Research Fund, with the financial support of Health Canada, National Institutes of Health (NIH R01 AG068563A, NIH R01 DA053301-01A1, NIH R01 MH129858-01A1), the Canadian Institute of Health Research (CIHR 438531, CIHR 470425), the Healthy Brains Healthy Lives initiative (Canada First Research Excellence fund) the IVADO R3AI initiative (Canada First Research Excellence fund), and by the CIFAR Artificial Intelligence Chairs programme (Canada Institute for Advanced Research). K.S. was

supported by the CIHR Brain Star Award (2023) and the Fonds de recherche Sante Doctorate Award (0000336637). We thank Ralph Adolphs for his comments throughout the project.

Author contributions

D.B. and K.S. conceived, executed and wrote the paper. B.T.T.Y, L.P. and J.D. contributed to the analysis and interpretation of the data, as well as revising the manuscript. D.B. led data analytics.

Competing interests

D.B. is a shareholder and advisory board member of MindState Design Labs, USA; as well as shareholder of Biossil, Canada. The remaining authors declare no competing interests.

Additional information

Supplementary information The online version contains supplementary material available at https://doi.org/10.1038/s41467-025-60451-8.

Correspondence and requests for materials should be addressed to Danilo Bzdok.

Peer review information *Nature Communications* thanks reviewer(s) Lu Zhao, Elisabeth Wenger, and Guy Vingerhoets for their contribution to the peer review of this work. A peer review file is available.

Reprints and permissions information is available at http://www.nature.com/reprints

Publisher's note Springer Nature remains neutral with regard to jurisdictional claims in published maps and institutional affiliations.

Open Access This article is licensed under a Creative Commons Attribution-NonCommercial-NoDerivatives 4.0 International License, which permits any non-commercial use, sharing, distribution and reproduction in any medium or format, as long as you give appropriate credit to the original author(s) and the source, provide a link to the Creative Commons licence, and indicate if you modified the licensed material. You do not have permission under this licence to share adapted material derived from this article or parts of it. The images or other third party material in this article are included in the article's Creative Commons licence, unless indicated otherwise in a credit line to the material. If material is not included in the article's Creative Commons licence and your intended use is not permitted by statutory regulation or exceeds the permitted use, you will need to obtain permission directly from the copyright holder. To view a copy of this licence, visit http://creativecommons.org/licenses/by-nc-nd/4.0/.

© The Author(s) 2025